

# "DIFFERENTIAL ACTIVATION OF GPCR SIGNALING PATHWAYS INVOLVED IN BRD4 ACTIVATION"

# **ASHIKA JAIN**

Co-supervised by Dr. Jason Tanny and Dr. Terence Hébert

Degree of Master of Science

Department of Pharmacology & Therapeutics

McGill University, Montreal, QC, Canada

December 2024

A thesis submitted to McGill University in partial fulfillment of the requirements of the degree of Master of Science

© Ashika Jain, 2024

#### **ACKNOWLEDGEMENTS**

Throughout this research I have received a great deal of support and guidance. I would like to express my gratitude to all those without whom this research work would not be possible.

First and foremost, I would like to extend my heartfelt gratitude to my supervisors, Dr. Jason Tanny and Dr. Terry Hébert, for giving me the opportunity to be part of their labs and for their unwavering belief in me. Their consistent support and encouragement have been invaluable, fostering my growth as a scientist and shaping my analytical thinking. They guided me through my degree, teaching me to approach challenges with resilience and grace. It was truly an honor to learn from such inspiring minds, which constantly fueled my curiosity and drive for learning. I could not have asked for better mentors.

I would like to thank the members of Hébert and Tanny labs for creating such a welcoming and supportive environment. Darlaine, Domo, Phan, Jana, Etienne, Kyla, Karima, Deanna, Robert, Alyson, Emma, Grace, Hanan, Aneesah, Giada, Deigo, Jenn, Viviane, Ali, Calvin, Peiran, Dorsa, Sana, thank you all for your constant support and encouragement throughout my journey. Thanks to Nico, for helping me navigate the instrumental facility with ease and for generously sharing his research insights, which provided valuable guidance along the way. I extend my gratitude to Jacob M. Blaney for his invaluable help in troubleshooting my experiments and sharing his experimental insights which greatly contributed to obtaining cleaner data. I am especially thankful to Andrew Bayne for his support and guidance during challenging times.

To the members of the Pharmacology admin team, Hong, Tina, Chantal, Cathy, Christiaan, for being an amazing team and working towards making a student experience memorable.

Thank you to my advisory committee, Dr. Bruce Allen, Dr. William Pastor and Dr. Jean-François Trempe for the guidance and for helping me navigate this journey with your expertise and knowledge.

I would also like to thank my friends outside the labs for always being there in times of need and were a huge part in my research journey, Ali, Calvin, Sabrina, Drashti, Anjan, Sanjana, Aayushi.

To my fiancé, Naitik Bhise, thank you for your unwavering support, patience, and encouragement throughout this journey. Your belief in me, especially during the challenging moments, has meant more than words can express. Thank you for being my steady source of strength and for always reminding me of my potential. I couldn't have done this without you by my side.

Finally, I am deeply grateful to my parents, grandparents, brother, and uncle for their unwavering love, support, and wisdom throughout my life. Their guidance and sacrifices have been instrumental in every step of my journey, providing me with the strength to pursue my education and build a meaningful future. From their encouragement during challenging times to their belief in my potential, they have given me the foundation and confidence to strive for my goals. I am truly blessed to have them as my pillars of strength, and I owe much of who I am today to their dedication and love.

# TABLE OF CONTENTS

ABST	RACT	6
RÉSU.	MÉ	8
CONT	RIBUTION OF AUTHORS	10
LIST (	OF ABBREVIATIONS	11
LIST (	OF FIGURES	13
INTRO	DDUCTION	15
1.1 Th	e role of GPCRs in cardiac remodeling processes in heart failure	15
1.2 Ca	rdiac Hypertrophy	16
1.2.1	Contractile Dysfunction	18
1.2.2 7	Franscriptional factors	19
1.3 Th	e BET family proteins: Key regulators of transcription and epigenetic control	20
1.3.1 E	Brd4-mediated regulation of general transcription	22
(A) P-	TEFb dependent pathways	22
(B) P-	TEFb independent pathways	24
1.4. Ta	argeting BET Proteins: Inhibitors and PROTACs	25
1.4.1 S	Small molecule inhibitors	25
1.4.2.	PROTACs	26
1.5. Di	ifferential activation of GPCR signaling pathways in cardiac hypertrophy	27
	READDs: A chemogenetic platform to specifically activate G protein signaling pathw	
	ale and objectives of this thesis	
	ERIALS AND METHODS	
2.1	Drugs	
2.1.1	Drug sources and stock concentrations	
2.1.2	Drug dilutions	
2.2	Plasmids	
2.3	Cell culture and transfection	
2.4	BRET measurements	
2.5	BRET analysis	
2.6	Protein extraction and Western blot	
2.7	RT-qPCR	
2.8	RNA isolation for RNA sequencing	
2.9	RNA seq analysis	39
RESU	LTS	41

3.1 Opt	imization of BET inhibitor treatment conditions	41
3.2. Act	tivation of Gas-coupled and Gaq-coupled DREADD receptors using DCZ	43
	nscriptomic Profiling of Gaq and Gas modulation in response to JQ1 and dBET6 ents via RNA Sequencing	46
	inscriptomic analysis of the effect of BET inhibitors on Gαs and Gαq-mediated gene ion	49
3.5. Ev	raluating the effect of BET inhibitors on Gαq receptor activation	54
3.6. Pat	hway Enrichment Analysis of genes modulated by BET inhibitors upon Gαq activation	
3.7. Eva	aluating the effect of BET inhibitors on Gαs activation	57
	SSION	
	ablishment of a DREADD-based system to monitor gene expression responses to Gαq s signaling	
4.1.1	Observations and challenges	60
4.1.2	Optimizing the DREADD system	61
4.2 Di	fferential gene expression upon Gαs and Gαq receptors activation	62
4.2.1.	BET inhibition and Brd4 dependency in Gαq- and Gαs-mediated gene activation	62
4.2.2	Distinct mechanisms of dBET6 and JQ1 in gene regulation	62
4.2.3	Comparison to prior lab findings in cardiac hypertrophy models	63
4.3. Ef	fects of BET Inhibitors on Inflammatory Pathways	63
4.3.1	Mechanisms of JQ1 and dBET6 in transcriptional regulation	64
4.3.2	Divergent effects of JQ1 and dBET6 on inflammatory pathways and c-myc Activation	64
4.3.3	Implications for BET Protein Function in Inflammatory Pathway Regulation	65
4.4. Co	onclusion and Implications of Brd4	66
FUTUR	RE DIRECTIONS	67
REFER	ENCES	69

#### **ABSTRACT**

Bromodomain-containing protein 4, an epigenetic reader protein and a member of the bromodomain and extra-terminal (BET) family of proteins, regulates key transcriptional pathways involved in cardiovascular diseases. BRD4 facilitates transcription by forming complexes with positive transcriptional elongation factor b (P-TEFb), Mediator, and other transcription factors. The BRD4 bromodomains interact with acetylated histones, and potentially other acetylated proteins; these interactions are important for BRD4 recruitment to chromatin. Small molecule inhibition of the interaction between BRD4 bromodomains and acetylated histones represses gene expression associated with pathologic cardiac hypertrophy and partially reverses previously established signs of heart failure. Using isolated cardiomyocytes, we previously showed that chromatin recruitment of BRD4 during pathologic hypertrophy depends on which G proteincoupled receptor (GPCR) signaling pathway initiates the hypertrophic response. GPCRs are the largest family of transmembrane receptors in eukaryotic cells and translate diverse extracellular signals into intracellular signaling cascades using heterotrimeric G proteins as adapters. GPCR signaling through the Gaq, G protein isoform is thought to be the major driver of the pathological hypertrophy response, but our work has shown that α<sub>1</sub>-adrenergic receptors can also stimulate hypertrophic response via cAMP/PKA pathway in a Gas-dependent manner. This pathway was more strongly linked to BRD4 activity, suggesting that there may be a general role for the  $G\alpha s/cAMP/PKA$ pathway in activating BRD4. This work aims to dissect the distinct GPCR signaling pathways that induce pathologic gene expression programs as it remains unclear how BRD4-dependent transcriptional responses are regulated in diseased conditions. Based on our previous data, we hypothesize that Gas and Gaq signaling pathways differentially activate BRD4-mediated gene expression. To investigate this, the aim of my project is to measure the BRD4-mediated gene expression downstream of Gaq and Gas signaling pathways using BET inhibitors, which competitively inhibit the interaction of BET bromodomains with acetyl lysine. Gas and Gaq signaling pathways were activated using Designer Receptors Exclusively Activated by Designer Drugs (DREADDs) in HEK 293 cells. RNA-seq analysis was performed to help us derive gene expression profiles following Gas and Gaq activation in the presence and absence of the BET inhibitors JQ1 and dBET6. It was found that Gαs-mediated genes were inhibited in presence of dBET6 whereas the same genes activated by Gaq were largely insensitive to JQ1 and dBET6, consistent with the idea that gene regulatory effects of  $G\alpha s$  signaling may rely more on BRD4 than those expressed by

G $\alpha q$ . Our data also suggested that G $\alpha q$ -activated genes upon BET inhibitor treatment did not suppress inflammatory pathways. Together, our results strengthen the idea that BRD4 activation is receptor-specific, with potential implications for understanding its role in inflammation and other cellular processes beyond heart disease.

# RÉSUMÉ

La protéine contenant un bromodomaine 4 (BRD4), une protéine lectrice épigénétique et membre de la famille des protéines BET (bromodomaine et extra-terminal), régule des voies transcriptionnelles clés impliquées dans les maladies cardiovasculaires. BRD4 facilite la transcription en formant des complexes avec le facteur d'élongation transcriptionnelle positive b (P-TEFb), le médiateur et d'autres facteurs de transcription. Les bromodomaines BRD4 interagissent avec les histones acétylées et potentiellement d'autres protéines acétylées; ces interactions sont importantes pour le recrutement de BRD4 à la chromatine. L'inhibition de petites molécules permettant l'interaction entre les bromodomaines BRD4 et les histones acétylées entraîne la réduction de l'expression génique associée à l'hypertrophie cardiaque pathologique et renverse partiellement les signes préétablis de l'insuffisance cardiaque. Par l'isolation de cardiomyocytes, nous avons démontré précédemment que le recrutement de BRD4 à la chromatine au cours de l'hypertrophie pathologique est dépendant du mécanisme de signalisation emprunté par les récepteurs couplés aux protéines G (RCPG) pour initier la réponse hypertrophique. Les GPCRs (récepteurs couplés aux protéines G) constituent la plus grande famille de récepteurs transmembranaires dans les cellules eucaryotes et traduisent divers signaux extracellulaires en cascades de signalisation intracellulaires en utilisant des protéines G hétérotrimériques comme adaptateurs. La signalisation des GPCRs via l'isoforme Gaq des protéines G est considérée comme le principal moteur de la réponse hypertrophique pathologique. Cependant, nos travaux ont montré que les récepteurs α1-adrénergiques peuvent également stimuler une réponse hypertrophique via la voie cAMP/PKA de manière dépendante de Gas. Ce mécanisme semble énormément lié à l'activité de BRD4 suggérant que le mécanisme G\u03c4s/cAMP/PKA pourrait avoir un rôle dans l'activation de BRD4. La présente étude vise à distinguer les mécanismes de signalisation reliés aux RCPGs qui induisent les programmes d'expression génique pathologique car il n'est pas connu de quelle façon les réponses transcriptionnelles dépendantes de BRD4 sont affectées lors de certaines maladies. Selon nos résultats antérieurs, nous émettons l'hypothèse que les mécanismes de signalisation de Gas et Gaq activent différemment l'expression génique médiée par BRD4. Pour étudier cela, l'objectif de mon projet est de mesurer l'expression génique médiée par BRD4 en aval des voies de signalisation  $G\alpha q$  et  $G\alpha s$  en utilisant des inhibiteurs de BET, qui inhibent de manière compétitive l'interaction des bromodomaines BET avec les lysines acétylées. Les inhibiteurs de BET ont été choisis car ils ciblent spécifiquement BRD4 et d'autres protéines de la famille BET, permettant d'inhiber l'activité transcriptionnelle médiée par BRD4 et de déterminer son rôle dans ces voies de signalisation. Les mécanismes de signalisation Gαs et Gαq ont été activés en utilisant des récepteurs artificiels exclusivement activés par des drogues de synthèse DREADDs) dans les cellules HEK293. Une analyse de séquençage de l'ARN a été faite pour obtenir des profils d'expression génique suivant l'activation de Gαs et Gαq lors de la présence ou l'absence des inhibiteurs BET, soit JQ1 et dBET6. Il a été constaté que les gènes médiés par Gαs étaient inhibés en présence de dBET6, tandis que les mêmes gènes activés par Gαq étaient largement insensibles à JQ1 et dBET6, ce qui est cohérent avec l'idée que les effets régulateurs de l'expression génique de la signalisation Gαs pourraient dépendre davantage de BRD4 que ceux exprimés par Gαq. Nos données ont également suggéré que les gènes activés par Gαq, après traitement par des inhibiteurs de BET, ne supprimaient pas les voies inflammatoires. Ensemble, nos résultats renforcent l'idée que l'activation de BRD4 est spécifique au récepteur, avec des implications potentielles pour comprendre son rôle dans l'inflammation et d'autres processus cellulaires au-delà des maladies cardiaques.

#### **CONTRIBUTION OF AUTHORS**

Dr. Dominic Devost contributed to the development of the BRET-based biosensors PKC and EPAC and designed the BRET bioassay protocol. Ms. Darlaine Pétrin contributed in the optimization of the transfection and the Maxi-prep protocols. Dr. Jennifer Chen and Dr. Ryan Martin generated the original scripts upon which the sequencing data processing and differential expression analysis in R were based. Dr. Jason Tanny created Figure 1.4A in this thesis. RNA sequencing and library preparation was performed by Genome Québec. Dr. Jason Tanny and Dr. Terry Hébert supervised the project and designed experiments.

Unless stated above, all work in this thesis was completed by Ashika Jain. This thesis was written by Ashika Jain and was co-edited by Dr. Jason Tanny and Dr. Terry Hébert. The French translation of the abstract was done by Ms. Viviane Pagé.

#### LIST OF ABBREVIATIONS

Brd4 Bromodomain-containing protein 4

BET Bromodomain and extra-terminal

SEC Secondary Elongation Complex

7SK snRNP 7SK small nuclear ribonucleoprotein

P-TEFb Positive Transcription Elongation Factor b

NELF Negative elongation factor

CTD C-terminal domain

PROTAC Proteolysis Targeting Chimera

DREADDs Designer Receptors Exclusively Activated by Designer Drugs

DCZ Deschloroclozapine

HEK Human embryonic kidney

CREM cAMP responsive element modulator

 $\alpha_1$ - adrenergic receptors

cAMP cyclic Adenosine Monophosphate

GPCR G protein-coupled receptors

GTP Guanosine diphosphate
GDP Guanosine triphosphate

1 1

ETR Endothelin receptors

PLC-β phospholipase C-β

DAG diacylglycerol

 $\alpha_1$ -AR

IP3 inositol trisphosphate

PKA Protein kinase A

PKC Protein kinase C

Pol II RNA polymerase II

LTCC L-type Ca<sup>2+</sup> channels

RyR2 Ryanodine receptors

EPAC Exchange Protein Directly Activated by cAMP

NFAT Nuclear Factor of Activated T-cells

GATA4 GATA Binding Protein 4

MEF2 Myocyte Enhancer Factor 2

HDAC Histone Deacetylase

HAT Histone Acetyltransferase

BRET Bioluminescence Resonance Energy Transfer

FRET Förster Resonance Energy Transfer

DMEM Dulbecco's Modified Eagle's Medium

DMSO Dimethyl sulfoxide

#### LIST OF FIGURES

- Figure 1.1. Pathologic Cardiac Remodeling and Progression to Heart Failure.
- **Figure 1.2** GPCR agonists drive cardiac hypertrophy through Gαq Signaling pathway.
- Figure 1.3 Structure of Brd4 and its bromodomains.
- **Figure 1.4.** Mechanism of P-TEFb Activation and Recruitment to Chromatin via Brd4.
- **Figure 1.5.** Brd4-mediated transcription mechanisms in three distinct stages.
- **Figure 1.6.** Induced degradation by BET PROTACS
- **Figure 1.7.** Differential activation of P-TEFb complexes via  $\alpha_1$ -AR and ETR in cardiac hypertrophy
- Figure 1.8. Structural and functional Basis of DREADD Activation by DCZ.
- **Table 1:** Drug concentration and dilution.
- Figure 3.1: Western blot and RT-qPCR analysis to confirm effects of BET inhibitors
- **Figure 3.2** BRET analysis of Gαq-DREADD and Gαs-DREADD activated using DCZ.
- **Figure 3.3.** BRET analysis of DCZ activation at longer time points.
- **Table 2:** Treatment conditions for G $\alpha$ q and G $\alpha$ s-coupled DREADD receptors for RNA seq.
- **Figure 3.4.** PCA plot for transcriptomic profiling of all the treatments
- **Figure 3.5:** Volcano plots depicting receptor activation.
- **Figure 3.6.** Volcano plots depict upregulated genes with and without the activation of indicated G protein.
- **Figure 3.7.** Venn Diagrams Comparing Two Treatments Highlighting Common and Distinct Gene Expression Patterns.
- **Figure 3.8.** KEGG pathway enrichment analysis highlighting key signaling pathways in the presence of inhibitors upon receptor activation
- Figure 3.9. Analyzing the effect of BET inhibitor on Gas Activation.

# Included in supplementary materials

- **Figure S1**. Quality Check of the DREADD Plasmids by Agarose Gel Electrophoresis.
- **Figure S2.** Western blot for optimization of dBET6 treatment.
- **Figure S3.** Comparative RT-qPCR analysis of c-myc levels following JQ1 and dBET6 treatment.

**Figure S4.** Comparative RT-qPCR analysis of c-myc levels following treatment with JQ1 and JQ1+DCZ.

*Appendix* – includes all the permission and licenses granted by the publications.

#### INTRODUCTION

# 1.1 The role of GPCRs in cardiac remodeling processes in heart failure

The heart is a muscular organ, intricately regulated to adapt and ensure optimal blood circulation under normal physiological conditions.<sup>1</sup> Heart disease is generally defined as any condition that impairs the ability of the heart to pump oxygenated blood to peripheral tissues and/or deoxygenated blood back to the lungs<sup>2</sup>. Heart diseases often arise from cardiac injuries like myocardial infarction, hypertension, diabetes, which can trigger cardiac remodeling processes in a healthy heart<sup>3</sup> (**Figure.1.1**). It remains one of the leading causes of death in Canada.<sup>4,5</sup> According to CCDSS (Canadian Chronic Disease Surveillance System), 1 in 12 Canadian adults aged 20 or older has been diagnosed with heart disease<sup>5,6</sup>. These pathologic remodeling processes eventually lead to heart failure, which accounts for approximately 32% of all deaths worldwide<sup>3,7,8</sup>.

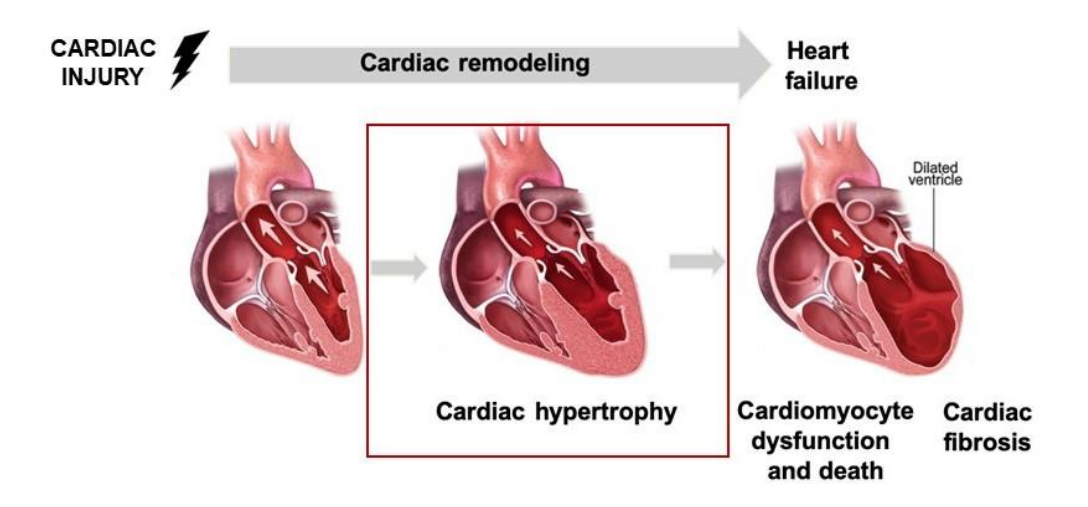


**Figure 1.1 Pathologic Cardiac Remodeling and Progression to Heart Failure.** Cardiac injuries such as myocardial infarction, contractile dysfunction, or arrhythmia can initiate prolonged cardiac remodeling, including cardiac hypertrophy. This remodeling can result in adverse outcomes like cardiomyocyte death and cardiac fibrosis, which further exacerbate the progression towards heart failure. Figure adapted from <sup>9</sup>

Cardiac remodeling processes refers to the changes in heart's shape, size and function to adapt to an injury or cardiac load<sup>10</sup>. Cardiac remodeling processes are driven by diverse signaling pathways which are activated via neurohormonal factors like catecholamines, angiotensin II, endothelin-1 which bind to specific membrane-bound G protein-coupled receptors (GPCRs)<sup>11–14</sup>. GPCRs are seven-transmembrane-spanning receptors coupled to heterotrimeric G proteins made

up of G $\alpha$  (including G $\alpha_q$ , G $\alpha_i$ , G $\alpha_s$ ) subunit and obligate heterodimer G $\beta\gamma^{15,16}$ . There are around 200 distinct GPCRs in the heart, and their signaling depends on the ligand that engages the receptor<sup>17</sup>. Upon ligand binding, typically at the receptor's N-terminal tail, extracellular loops, or exofacial transmembrane helices, GPCRs undergo a conformational change<sup>18</sup> <sup>16</sup>. This activates the associated G-protein by exchanging GDP for GTP on the G $\alpha$  subunit, causing its dissociation from the G $\beta\gamma$  dimer<sup>16,18</sup>. The G $\alpha$  subunit then triggers specific downstream signaling pathways depending on its type (G $\alpha$ s, G $\alpha$ i, G $\alpha$ q, or G $\alpha$ 11/12), each leading to different physiological responses<sup>16,18</sup>.

# 1.2 Cardiac Hypertrophy

Physiological cardiac hypertrophy is a stress-adaptive response that helps the heart manage increased demands during activities such as exercise, pregnancy, or post-natal development. <sup>19,20</sup>. However, in response to pathological stimuli such as pressure overload, G protein-coupled receptors (GPCRs) are activated by neurohormonal factors like angiotensin II (Ang II), endothelin-1 (ET-1), and norepinephrine (NE). These factors promote cardiac growth by binding to their respective GPCRs: Ang II interacts with the AT1 receptor, ET-1 binds to endothelin receptors (ETA and ETB), and NE engages  $\alpha_1$ -adrenergic receptors (ARs)<sup>11–14,21</sup>. Upon ligand binding, these receptors activate the  $G\alpha q/11$  protein, which stimulates phospholipase C- $\beta$  (PLC- $\beta$ ). This activation leads to the production of diacylglycerol (DAG) and inositol trisphosphate (IP3), triggering downstream signaling pathways<sup>22</sup> (**Figure 1.2**).

The hypertrophic response induced by GPCR agonists involves a common signaling cascade via  $G\alpha q/11$  and PLC- $\beta$ , which plays a critical role in the development of hypertrophy under pathological conditions<sup>23,24</sup>. The significance of  $G\alpha q/11$  signaling is further highlighted by studies on transgenic mice: overexpression of  $G\alpha q$  in the heart leads to hypertrophy and dysfunction, while disruption of  $G\alpha q/11$  signaling protects against hypertrophy even under stress<sup>25,26</sup>. Together, these findings indicate a pivotal role of  $G\alpha q/11$  in mediating pathological cardiac growth, making it a key target for therapeutic interventions aimed at preventing heart failure<sup>25,26</sup>.

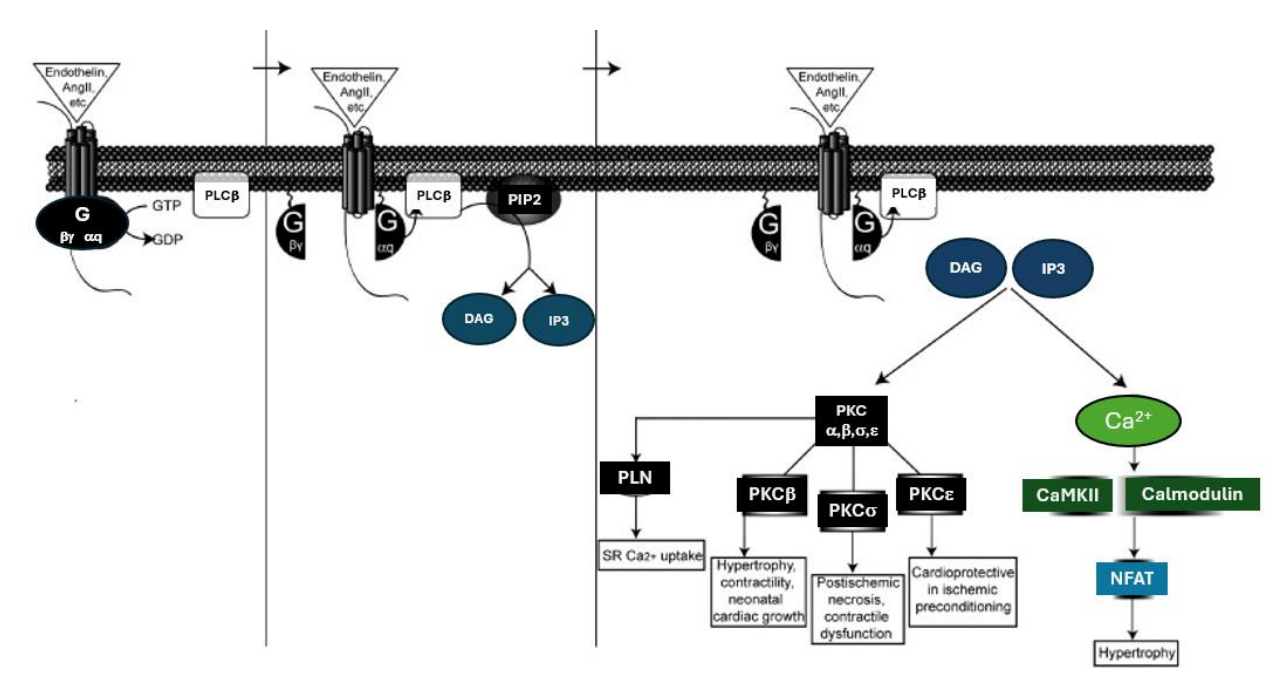


Figure 1.2. GPCR agonists drive cardiac hypertrophy through  $G\alpha q$  Signaling pathway. DAG activates various isoforms of protein kinase C (PKC), including PKCβ, PKCα, and PKCε. These PKC isoforms regulate different cardiac processes: PKCβ is associated with hypertrophy and neonatal cardiac growth, PKCα contributes to contractile dysfunction, while PKCε plays a cardioprotective role in ischemic preconditioning. Meanwhile, IP3 elevates intracellular calcium levels, activating calcium-dependent pathways such as CaMKII and NFAT, both of which contribute to hypertrophic signaling. Figure adapted from  $^{27}$ .

Reprinted by permission from Elsevier publishers, Natasha C. Salazar, Juhsien Chen, Howard A. Rockman, "Cardiac GPCRs: GPCR signaling in healthy and failing hearts", Biochimica et Biophysica Acta (BBA) - Bio membranes, Volume 1768, Issue 4, Copyright 2007,

Pathologic cardiac hypertrophy is characterized by thickening of the ventricular wall, increased size of cardiomyocytes accompanied by accumulation of myocardial collagen, myocyte elongation (eccentric hypertrophy), serial assembly of sarcomeres and reinduction of a fetal gene expression program<sup>19,28</sup>. The reinduction of this fetal gene expression program includes the upregulation of genes encoding the natriuretic peptides and the switch between the two myosin chain (MHC) isoforms,  $\alpha$  and  $\beta$  <sup>29</sup>.

## 1.2.1 Contractile Dysfunction

The heart's ability to circulate blood throughout the body is facilitated by the synchronized contraction (systole) and relaxation (diastole) of cardiomyocytes, which together comprise the cardiac cycle<sup>30</sup>. During systole, the depolarization of the cardiomyocyte triggers the opening of voltage-gated L-type Ca<sup>2+</sup> channels (LTCC), allowing Ca<sup>2+</sup> influx into the cell<sup>31,32</sup>. This influx activates ryanodine receptors (RyR2) on the sarcoplasmic reticulum (SR), leading to the release of SR-stored Ca<sup>2+</sup> into the cytosol<sup>31,32</sup>. The resulting increase in cytoplasmic Ca<sup>2+</sup> concentration activates contractile proteins in the sarcomere, driving ATP-dependent contraction of the cardiomyocyte<sup>40,41</sup>. Following contraction, diastole is facilitated by the removal of Ca<sup>2+</sup> from the cytoplasm. This process is largely regulated by SERCA2a (sarco-/endoplasmic reticulum Ca<sup>2+</sup>-ATPase 2a), which pumps Ca<sup>2+</sup> back into the SR to maintain proper calcium handling<sup>32</sup>. In pathologic conditions such as hypertrophic and failing hearts, SERCA2a expression and activity are downregulated, which leads to accumulation of Ca<sup>2+</sup> in cytoplasm<sup>31</sup>. This results in increased cytosolic Ca<sup>2+</sup> levels during diastole and a reduction in SR Ca<sup>2+</sup>content, ultimately contributing to contractile dysfunction and heart failure<sup>33–35</sup>.

In pathological conditions like hypertrophy or heart failure, these regulatory processes are significantly impaired. Protein kinase A (PKA), a crucial regulator of cardiac function and structural activity, is often found to be abnormal in pathological conditions thereby causes contractile dysfunction, as it plays a vital role in excitation-contraction coupling in cardiomyocytes<sup>36,37</sup>. Notably, PKA-mediated hyperphosphorylation of the ryanodine receptor/Ca<sup>2+</sup> release channel has been observed in the hearts of transgenic mice, resulting in elevated expression levels of hypertrophic gene markers such as ANP and BNP <sup>38</sup>. One of the hallmarks of pathologic cardiac remodeling is the shift in the relative expression levels of  $\alpha$ -MHC and  $\beta$ -MHC, as observed in rodent models <sup>39-41</sup>. During early developmental stages,  $\beta$ -MHC is expressed at higher levels than  $\alpha$ -MHC<sup>39,42,43</sup>. However, with advancing age, this pattern shifts, and  $\alpha$ -MHC becomes the more dominant isoform. In rodent hearts under pathophysiological state, similar expression patterns have been observed <sup>39</sup>. Since  $\alpha$ -MHC exhibits higher actin-activated ATPase activity than  $\beta$ -MHC, this results in increased myofiber shortening velocity, ultimately contributing to contractile dysfunction. <sup>39,44,45</sup>. Furthermore, genes encoding natriuretic peptides, such as atrial natriuretic peptide (protein encoded by *Nppa*) and B-type natriuretic peptide (protein

encoded by Nppb), serve as common markers for pathologic cardiac hypertrophy and are upregulated in a manner similar to that seen in fetal hearts<sup>46–48</sup>.

# 1.2.2 Transcriptional factors

Epigenetic regulation is a dynamic process managed by three primary regulators: writers, readers, and erasers. Epigenetic writers, such as histone acetyltransferases (HATs), introduce modifications like acetylation on histones, thereby influencing gene expression patterns. These modifications are recognized by specialized protein modules known as epigenetic readers, such as bromodomains, which detect and bind specific acetylation marks, further influencing chromatin structure and function<sup>49,50</sup>. Conversely, epigenetic erasers, such as histone deacetylases (HDACs), remove these modifications, thereby maintaining the dynamic regulation of epigenetic states<sup>51,52</sup>. Two classes of HDACs have been extensively studied in connection with heart disease and cardiac hypertrophy: class I HDACs, which are constitutively nuclear and reside in large transcriptional repressor complexes; and class II HDACs, which shuttle between cytoplasm and nucleus in response to stimuli<sup>53–55</sup>.

In context of cardiac hypertrophy, a key transcription factors is NFAT, which is dephosphorylated by the calcium- and calmodulin-dependent phosphatase calcineurin<sup>56</sup>. This dephosphorylation enables the nuclear translocation of NFAT, facilitating its interaction with other hypertrophic transcription factors like MEF2 and GATA4<sup>28,57</sup>. This interaction promotes the transcription of hypertrophic genes. Calcineurin increases nuclear accumulation of MEF2, partly due to the stress-induced shuttling of class IIa HDACs between the nucleus and the cytoplasm<sup>58,59</sup>. When nuclear export of class IIa HDACs occurs, it releases MEF2 from repression, allowing MEF2 to bind HATs, thereby increasing histone acetylation and promoting cellular growth<sup>58,59</sup>.

Class IIa HDACs play a particularly selective role in modulating MEF2 activity. They interact with MEF2 through an 18-amino-acid motif unique to these HDACs, forming repressive complexes on gene regulatory elements at MEF2 binding sites<sup>59</sup>. Studies have shown that in HDAC-knockout animals, MEF2 activity is significantly increased, indicating a direct link between class IIa HDACs and MEF2-mediated transcription in cardiac pathology<sup>60</sup>. During stress, however, class IIa HDACs relocate to the cytoplasm, releasing MEF2 and allowing it to recruit HATs. This recruitment leads to increased histone acetylation at specific hypertrophic gene loci, further driving the transcription of genes related to cellular growth and hypertrophy<sup>58,59</sup>.

Although the roles of HAT inhibitors in cardiac remodeling are not fully elucidated, certain HATs, like p300, have been shown to induce dilated cardiomyopathy in animal models<sup>61</sup>. HDAC inhibitors have been found to significantly suppress agonist-induced cardiac hypertrophy, despite increasing histone acetylation<sup>62,63</sup>. This paradoxical effect likely arises from HDAC inhibitors blocking the phosphorylation-dependent shuttling of class IIa HDACs, which normally suppress hypertrophy by blocking HAT binding to MEF2 and other transcription factors<sup>64</sup>. Additionally, these inhibitors may target class I HDACs, which are implicated in activating genes that promote cell growth, thereby reducing hypertrophic signaling and contributing to the antihypertrophic effect<sup>28,64</sup>.

# 1.3 The BET family proteins: Key regulators of transcription and epigenetic control

Epigenetic reader molecules are proteins that recognize various post-translational modifications on histone tails, including N-ε-acetylation of lysine side chains, which is often associated with transcriptional activation<sup>50,65</sup>. Many epigenetic reader molecules contain acetyllysine recognition domains, or bromodomains, which are approximately 110 amino acids in length. In humans, these bromodomains are present a total of 61 times across 46 diverse proteins<sup>50,66,67</sup>.

Bromodomain-containing proteins consists of four  $\alpha$  helices ( $\alpha_Z,\alpha_A,\alpha_B,\alpha_C$ ) connected by 2 loops (ZA and BC) which forms a central hydrophobic cavity that recognizes acetyl lysine residues (**Figure 1.3**)<sup>68</sup>. Bromodomain-containing proteins have been implicated in various diseases like cancer, neurological diseases, inflammatory diseases, and cardiovascular diseases 69,70

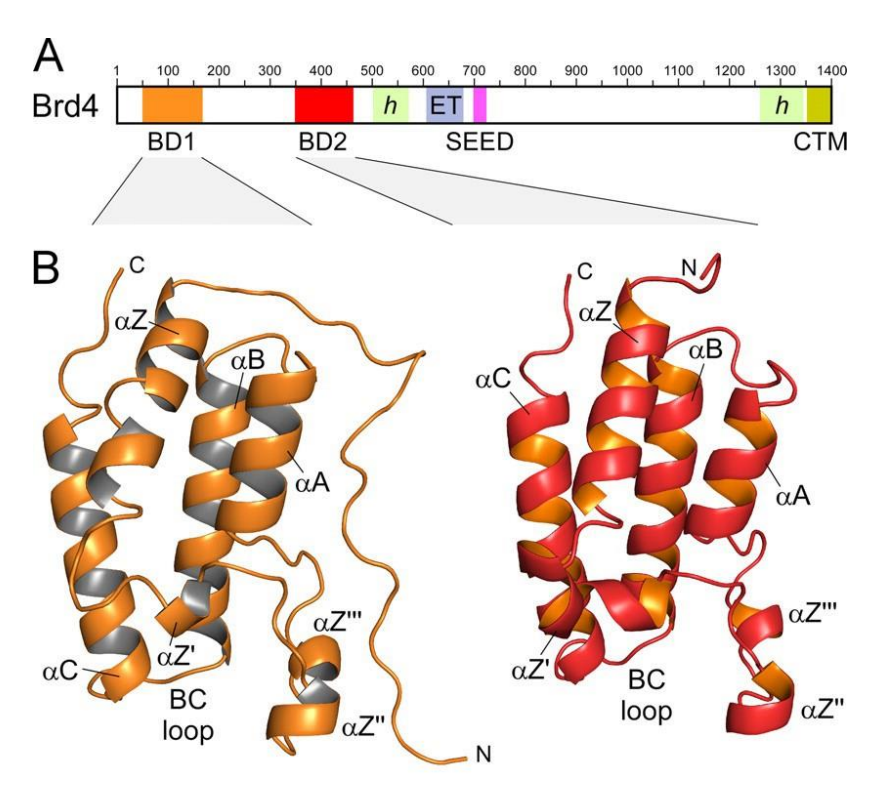


**Figure 1.3. Structure of Brd4 and its bromodomains.** (**A**) Schematic domain architecture of Brd4, highlighting two bromodomains (BD1 and BD2) and other functional regions such as extra terminal domain (ET) followed by SEED which denotes a serine-, glutamate-, and aspartate-rich region. Brd4 also has a conserved C-terminal motif (CTM). The green 'h' marks indicate helicase-like regions, and the ET domain is known to mediate interactions with other transcription factors<sup>71</sup>. (**B**) crystal structure of Brd4's bromodomains. Each bromodomain consists of four α-helices ( $\alpha Z$ ,  $\alpha A$ ,  $\alpha B$ ,  $\alpha C$ ) and two interconnecting loops, ZA and BC. The ZA loop connects  $\alpha Z$  and  $\alpha A$  helices which contains three short helices ( $\alpha Z$ ',  $\alpha Z$ ", and  $\alpha Z$ "). The BC loop connects the  $\alpha B$  and  $\alpha C$  helices. These loops (ZA and BC) together form a deep cleft, constituting a recognition site for binding acetylated lysines on histone tails, which is essential for Brd4's role in chromatin targeting and transcription regulation<sup>71</sup>. Figure adapted from <sup>71</sup>

Bromodomain extra-terminal (BET) family proteins include Brd2, Brd3, Brd4 and BrdT, which share a similar architecture with highly conserved amino-terminal bromodomains and an extra-terminal domain <sup>50,68</sup>. Brd4 is known to be involved in transcriptional regulation by forming a complex with the positive transcriptional elongation factor, P-TEFb <sup>72,73</sup>. P-TEFb is a heterodimeric elongation factor which consists of the cyclin-dependent kinase Cdk9 and its cyclin partner CyclinT1. Its kinase activity is known to promote RNA polymerase II (Pol II) – mediated elongation <sup>74</sup>. Brd4 and BrdT have a C-terminal domain not found in Brd2 or Brd3 that mediates interaction with P-TEFb <sup>75</sup>. Whereas BrdT is testis-specific and relatively poorly characterized, Brd4 has been established as a major transcriptional co-activator in many physiological settings.

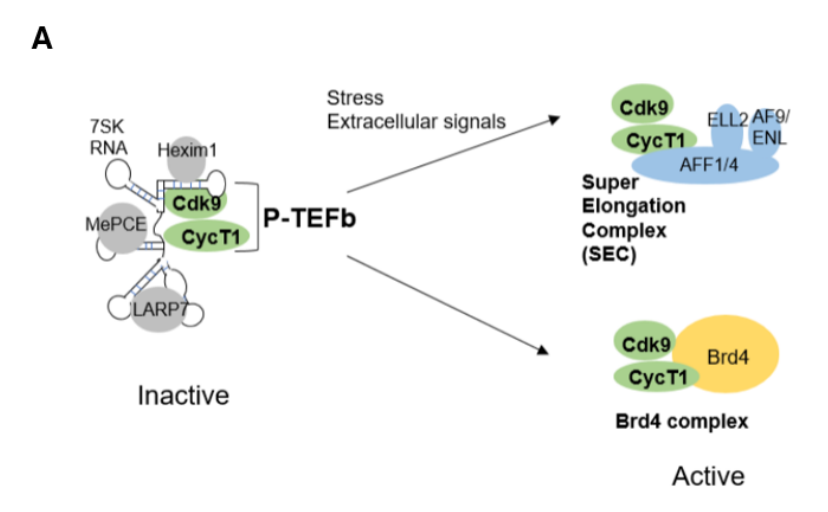
Studies have shown that the C-terminal domain of Brd4 interacts directly with Cyclin T1 and Cdk9<sup>76,77</sup>. Meanwhile, the canonical function of bromodomains (BDs) is to bind acetylated histones, anchoring BET proteins to chromatin and facilitating their role in regulating gene transcription <sup>72,75</sup>. BET family proteins also interacts with a multi-protein coactivator known as the Mediator complex which binds to transcription factors and further activates RNA Polymerase II

# 1.3.1 Brd4-mediated regulation of general transcription

## (A) P-TEFb dependent pathways

Brd4 is a pivotal regulator in both cardiac pathogenesis and general transcription. It plays a key role in transcription elongation by recruiting positive transcription elongation factor b (P-TEFb) to the proximal promoter regions of genes, facilitating the transition from transcription initiation to productive elongation<sup>79</sup>. P-TEFb functions with three major interacting partners: Brd4, the super elongation complex (SEC), and the 7SK small nuclear ribonucleoprotein (7SK snRNP)<sup>79,80</sup>. The 7SK snRNP complex, which includes the 7SK RNA, sequesters P-TEFb in its inactive state, preventing premature transcription elongation. In this inactive complex, P-TEFb's kinase activity is suppressed, allowing for tight regulation of its activation<sup>79,80</sup>.

Upon stimulation by stress or extracellular signals, P-TEFb is released from 7SK snRNP and forms active complexes with Brd4 and the SEC. These complexes recruit P-TEFb to transcriptionally paused regions, where it phosphorylates key transcriptional regulators, including the C-terminal domain (CTD) of RNA polymerase II (Pol II), the negative elongation factor (NELF), and the DRB sensitivity-inducing factor (DSIF)<sup>72,74,81</sup> (**Figure 1.4A**). Phosphorylation of NELF and DSIF promotes the dissociation of NELF from Pol II and converts DSIF from a repressor to an activator, enabling Pol II to escape promoter-proximal pausing and transition into productive elongation (**Figure 1.4B**)<sup>74</sup>. Formation of the P-TEFb-Brd4 complex further stabilizes P-TEFb in its active form and facilitates its release from the 7SK snRNP complex<sup>79,80</sup>.



В

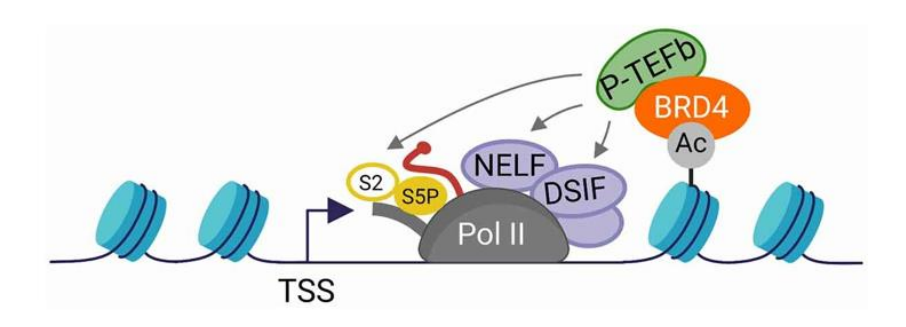


**Figure 1.4. Mechanism of P-TEFb Activation and Recruitment to Chromatin via Brd4.** (**A**) In the inactive state, P-TEFb is sequestered by 7SK snRNP, while extracellular stress signals trigger its release and activation, allowing P-TEFb to associate with Brd4 or SEC. (**B**) the role of P-TEFb in transcriptional regulation, specifically its Brd4-mediated recruitment to chromatin. P-TEFb phosphorylates key targets, including Ser2 of the RNA Polymerase II C-terminal domain (CTD), NELF, and DSIF (depicted by grey arrows), promoting transcriptional elongation at the transcription start site (TSS). Figure adapted from <sup>82</sup>

Brd4 binding to P-TEFb is known to compete with HIV-1 Tat regulatory protein, making the Brd4-P-TEFb interaction inhibitory to HIV-1 transcription<sup>83</sup>. Brd4-P-TEFb complex formation is also known to trigger the transcription of NF- $\kappa$ B-responsive inflammatory genes since Brd4 interacts with the RelA subunit of NF- $\kappa$ B<sup>84</sup>. The bromodomains of Brd4 recognize and binds to acetylated lysine-310 on RelA<sup>85</sup>. This interaction activates the transcriptional activity of NF- $\kappa$ B,

thereby promoting an inflammatory response<sup>84</sup>. Thus, Brd4 plays a critical role in the regulation of NF-κB-dependent inflammatory gene expression<sup>85–87</sup>.

Brd4's transcription regulation extends to its interaction with histone modifiers through its ET domain, including JMJD6 (an arginine demethylase) and NSD3 (a lysine methyltransferase), both of which contribute to transcriptional pause release<sup>88,89</sup>. Additionally, ET domain interacts with chromatin remodelers such as SWI/SNF and CHD2<sup>89</sup>. Brd4 also associates with various chromatin-modifying enzymes and transcription factors, including p53, YY1, AP2, c-Jun, c-Myc/Max, C/EBPα, C/EBPβ, Acf1, and G9a<sup>90,91</sup>.

# (B) P-TEFb independent pathways

Brd4 regulates transcription through both P-TEFb-dependent and P-TEFb-independent mechanisms. In addition to its well-known role in recruiting P-TEFb to facilitate transcription elongation, Brd4 independently regulates transcription by co-localizing with the Mediator complex along cis-regulatory genomic regions 92–94.

The Mediator complex itself is a large coactivator composed of 26 subunits in mammals, known to interact with transcription factors to mediate the recruitment and activation of RNA polymerase II (Pol II) (**Figure 1.5**) <sup>96</sup>. Brd4 co-localizes with the Mediator complex at cisregulatory genomic regions to facilitate the assembly of the pre-initiation complex (PIC)<sup>95</sup>. Studies have shown that BET bromodomain inhibition by JQ1 displaces Brd4 from chromatin, leading to reduced Mediator occupancy at cis-regulatory elements<sup>95</sup>. This indicates that Brd4 plays a crucial role in the recruitment and stabilization of Mediator at these sites<sup>97,98</sup>.

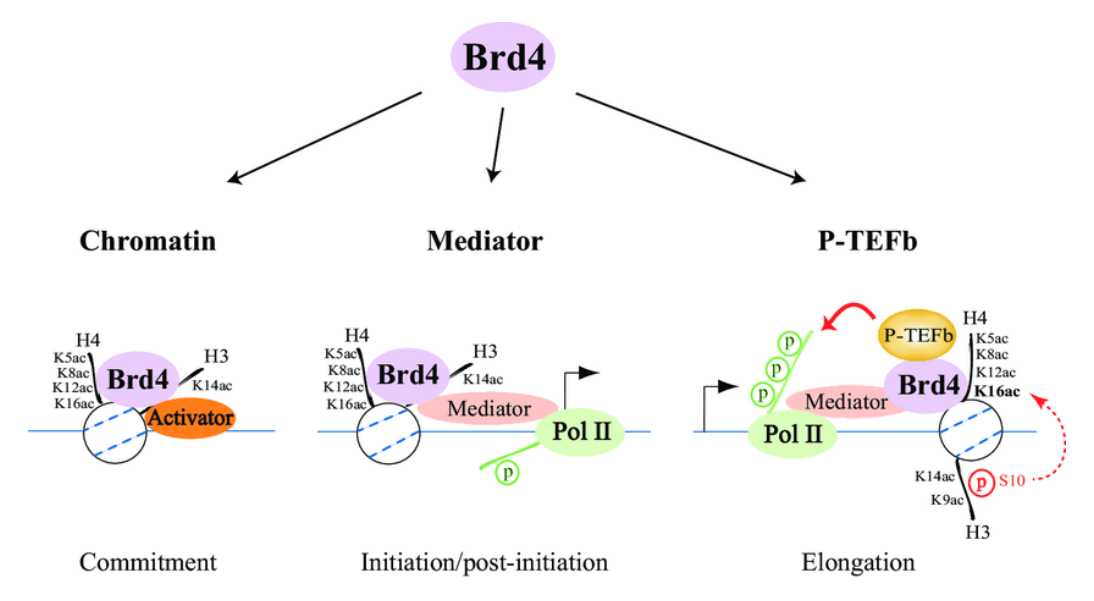


Figure 1.5. Brd4-mediated transcription mechanisms in three distinct stages.

- (1) Commitment to Transcription: In the initial stage, Brd4 cooperates with transcription factors to bind target gene loci. Brd4's tandem bromodomains recognize and interact with acetylated histones, specifically acetylated lysines (K5ac, K8ac, K12ac, K16ac) on histone H4 and acetylated lysine 14 (K14ac) on histone H3<sup>99</sup>.
- (2) **Initiation and Post-Initiation:** At this stage, Brd4 recruits the Mediator complex, which serves as a bridge between transcription factors and RNA polymerase II (Pol II). This recruitment facilitates phosphorylation of the Pol II carboxyl-terminal domain (CTD) at Ser5, an essential step for transitioning from transcription initiation to post-initiation. Brd4 colocalizes with mediator complex, ensuring that the pre-initiation complex (PIC) is assembled, and transcription is properly activated<sup>99</sup>.
- (3) **Elongation:** Brd4 promotes the recruitment of P-TEFb (positive transcription elongation factor b) to pause Pol II transcription. This step leads to the phosphorylation of the Pol II CTD at Ser2, enabling transcription elongation to proceed. Additionally, Brd4's recruitment to acetylated nucleosomes downstream of the transcription start site involves crosstalk between acetylated lysine 9 (K9ac) and phosphorylated serine 10 (S10) on histone H3, and H4K16ac. These histone modifications allow Brd4 to regulate the elongation phase of transcription<sup>99</sup>. Figure adapted from <sup>99</sup>.

#### 1.4. Targeting BET Proteins: Inhibitors and PROTACs

#### 1.4.1 Small molecule inhibitors

The BET family has become a key target for small-molecule drug discovery, with several inhibitors advancing to clinical trials for various cancers<sup>100</sup>. These inhibitors work by blocking the BD-acetyl-lysine interaction thereby preventing chromatin recruitment. Small molecule BET inhibitors are widely used due to its high affinity for bromodomains in BET family proteins <sup>66,101</sup>. In 2010, along with JQ1, another group had reported I-BET to be a promising small-molecule

inhibitor with similar chemical structure as JQ1 <sup>102,103</sup>. JQ1 and I-BET were the first pan-BET inhibitors, with affinities of 50-90 nM and 50.5-61.3 nM for Brd4 bromodomains 1 and 2, respectively <sup>102,103</sup>. JQ1 reduced proliferation in NUT midline carcinoma models <sup>102</sup> while I-BET blocked LPS-induced inflammation in macrophages <sup>103</sup>. BET inhibitors has also shown promising results for treating hematological cancers, solid tumors, rheumatoid arthritis, and heart failure <sup>104–107</sup>

The BET family proteins play a central role in pathologic cardiac remodeling processes as well <sup>108,109</sup>. BET protein expression levels accessed in neonatal rat ventricular cardiomyocytes (NRVMs) and adult mouse ventricular tissue revealed that Brd4 is the most highly expressed BET family proteins in heart <sup>108</sup>. To further confirm the significance of Brd4 in transcriptional elongation in cardiac remodeling, small molecule BET inhibitor like JQ1 have been used <sup>108,110,111</sup>. Phenylephrine-induced hypertrophy in NRVMs was attenuated by JQ1 and it also reduced hypertrophy induced via pressure overload mediated by transverse aortic constriction (TAC) in mice model <sup>104,108,109,112</sup>. JQ1 was also found to repress gene expression associated with pathologic hypertrophy in both agonist-induced hypertrophic NRVMs and TAC-mediated mice model <sup>108,109</sup>. In hypertrophic mouse model, Brd4 inhibition was able to partially reverse previously established signs of heart failure <sup>104</sup>. Brd4 inhibition leads to loss of Brd4 occupancy from super enhancers and promoters of hypertrophic genes in cardiomyocytes <sup>111,112</sup>.

Overall, these observations indicate that inhibition of Brd4 and BET proteins can effectively suppress pathologic cardiac remodeling and potentially provide a therapeutic approach for heart failure and other related conditions.

#### 1.4.2. PROTACs

PROTACs represent a strategy for targeted protein degradation and are composed of a hetero-bifunctional molecule that contains two key functional groups: one ligand binds to the target protein (e.g., Brd4), while the other binds to an E3 ubiquitin ligase, like cereblon, recruiting the ligase to the target protein and marking it for degradation) <sup>97</sup> (**Figure 1.6**). In cancer, cereblon-based PROTACs have been found to efficiently target Brd4, showing potential advantages over small-molecule inhibitors. One such highly permeable BET protein degrader is dBET6; however, its effects remain to be explored in cardiovascular disease.

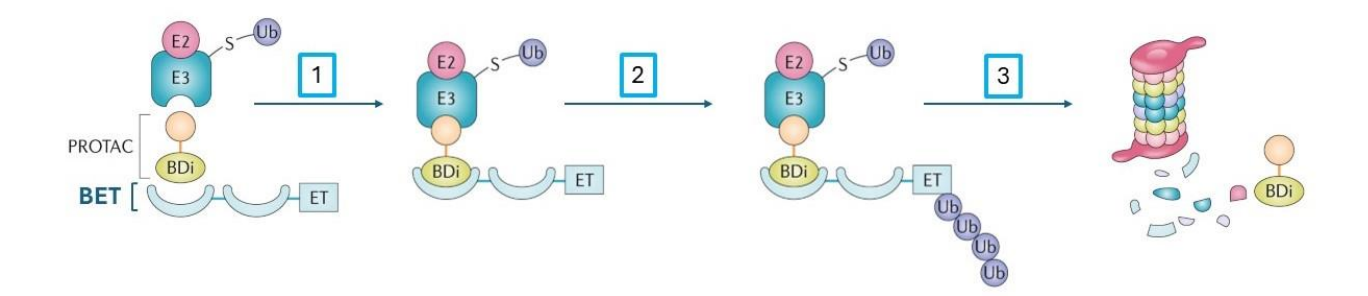


**Figure 1.6. Induced degradation by BET PROTACS.** This process highlights how PROTACs facilitate the targeted degradation of BET proteins via the ubiquitin-proteasome pathway.

PROTAC is made up of a Protein of interest (POI) (green oval) ligand covalently linked to a suitable E3 ligand (natural degron or synthetic analogue, depicted as an orange circle). Bromodomain inhibitor (BDi) can be used as an E3 ligand that engages with the E3 ubiquitin ligase, whereas the POI targets the protein that is to be degraded<sup>66</sup>. Following ubiquitin activation by E1 and transfer to E2 (not shown), a three-step ubiquitin-mediated proteolysis occurs:

Step 1: Substrate-E3-E2-Ub complex formation: The PROTAC links the BET protein to the E3 ubiquitin ligase, forming a ternary complex. The E2 enzyme transfers ubiquitin (Ub) to the BET protein, marking the start of ubiquitination<sup>66,97</sup>.

*Step 2: Ubiquitin chain addition:* The E3 ligase catalyzes the polyubiquitination of the BET protein by attaching multiple ubiquitin molecules to its lysine residues, forming a polyubiquitin chain<sup>66,97</sup>.

Step 3: Proteasomal degradation: The polyubiquitinated BET protein is recognized and degraded by the 26S proteasome, while the PROTAC molecule is released and can be reused<sup>66</sup>. Figure adapted from <sup>66</sup> Reprinted by permission from Springer Nature publishers, Cochran, A.G., Conery, A.R. & Sims, R.J.

"Bromodomains: a new target class for drug development", Nat Rev Drug Discov 18, 609-628 Copyright 2019.

# 1.5. Differential activation of GPCR signaling pathways in cardiac hypertrophy

GPCRs stimulate cardiac hypertrophy classically via G $\alpha$ q, but our prior lab studies have shown that  $\alpha_1$ -adrenergic receptors can stimulate hypertrophic response via cAMP/PKA pathway in a G $\alpha$ s-dependent manner <sup>113</sup>. To confirm that GPCR activates cAMP signaling in a G $\alpha$ s-dependent manner, distinct signaling pathway responses following the activation of  $\alpha_1$ -adrenergic receptors and endothelin receptors (ETR) were analyzed via RNA-seq analysis in rat neonatal cardiomyocytes following receptor stimulation <sup>113</sup>. CREM (cAMP responsive element modulator) expression levels were strongly upregulated upon 1.5 hr. activation of  $\alpha_1$ -adrenergic receptors but not after ETR activation <sup>113</sup>. Previous studies have shown activation of  $\alpha_1$ -adrenergic receptors coupled to G $\alpha$ s to activate adenylyl cyclase (AC) which causes cAMP accumulation, leading to

PKA activation  $^{114-117}$ . Our work has also confirmed the cAMP accumulation downstream of both  $\alpha_{1A}$ - and  $\alpha_{1B}$ -AR receptors using BRET-based EPAC biosensors which were transfected in HEK 293 cells  $^{113}$ . Further, FRET-based PKA biosensors with NES (nuclear export sequence) or NLS (nuclear localization sequence) were used in HEK 293 cells to observe differential activation of PKA upon stimulation by  $\alpha_{1A}$ - and  $\alpha_{1B}$ -AR receptors  $^{113}$ . It was confirmed that both  $\alpha_{1}$ -AR subtypes stimulate nuclear PKA activity in a G $\alpha$ s-dependent manner  $^{113}$ .

Hypertrophy-associated gene expression and phenotypic changes in cardiomyocytes are critically regulated by P-TEFb, as validated in models of cardiac-specific Gaq overexpression in mice and ETR stimulation in NRVMs. 118. Pathologic transcriptional events following hypertrophy is dependent on the recruitment of P-TEFb via Brd4 or via interactions with SEC <sup>119</sup>. Our previous lab studies have also demonstrated the differential activation of P-TEFb via its interacting partners, SEC and Brd4 in cardiac hypertrophy upon activation of  $\alpha_1$ -AR and ETR <sup>119</sup>(**Figure 1.6**). These findings were validated using high-content microscopy which showed an increase in cardiomyocyte area upon 24hr treatment with both PE (agonist for  $\alpha_1$ -AR) and ET-1 (agonist for ETR) <sup>119</sup>. Furthermore, effects of hypertrophic inducers on gene expression were validated using RT-qPCR where it was found that mRNA levels of established hypertrophic gene markers i.e. Nppa, Nppb and Serpine1 were upregulated. However, it was found that SEC knockdown attenuated hypertrophy induced by both  $\alpha_1$ -AR and ETR agonists whereas BET inhibition with JQ1 decreased hypertrophy induced via  $\alpha_1$ -AR but had no effect on hypertrophy induced by ETR agonist <sup>119</sup>. These results suggested that P-TEFb-SEC is generally required in hypertrophy and P-TEFb-Brd4 complex mediates a receptor-specific response <sup>119</sup> (**Figure 1.7**). Further, cardiomyocyte mRNA expression patterns were assessed upon PE and ET-1 treatment and upregulated genes were further characterized using Ingenuity pathway analysis (IPA) <sup>119</sup>. This suggested an increased activity of all hypertrophic transcription factors including NFkB, Jun, Fos, GATA4 upon activation of either receptor <sup>90,119</sup>. In addition to the previous results, JQ1 specifically attenuated PE-induced hypertrophic transcription factor activity. This suggested that  $\alpha_1$ -AR receptor signaling, but not ETR signaling, increased hypertrophic transcription factor activity in a Brd4-dependent manner <sup>119</sup>.

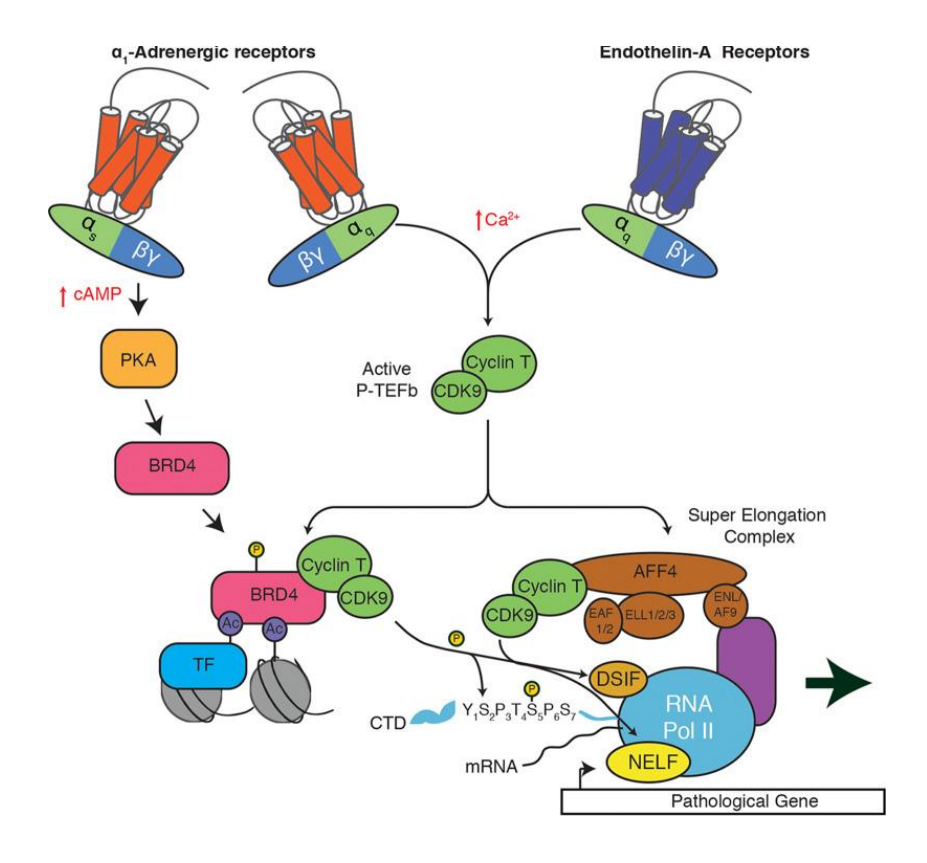


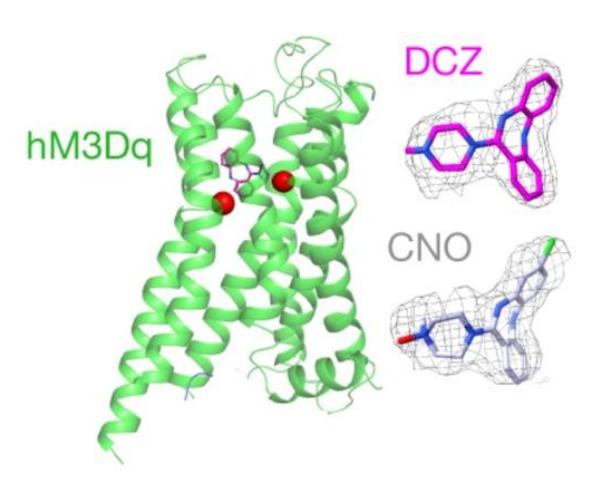
Figure 1.7. Differential activation of P-TEFb complexes via  $\alpha_1$ -AR and ETR in cardiac hypertrophy.  $\alpha_1$ -Adrenergic receptors activate the cAMP/PKA pathway, leading to B4-mediated recruitment of P-TEFb, while Endothelin-A receptors increase calcium levels, activating P-TEFb through the Super Elongation Complex. Both pathways result in phosphorylation of RNA polymerase II, promoting transcription of hypertrophic genes<sup>119</sup>. Figure adapted from <sup>119</sup>.

Our previously published work confirmed  $\alpha_1$ -adrenergic receptors to activate cAMP/PKA pathway in a G $\alpha$ s-dependent manner <sup>113</sup>. Therefore, to investigate if G $\alpha$ s/PKA pathway is critical to activate Brd4 function in cardiac hypertrophy, ChIP-qPCR was used to quantify Brd4 localization in previously defined promoters and super enhancers <sup>112,119</sup>. This analysis was performed in NRVMs treated with selective PKA inhibitor, KT5720 <sup>119</sup>. It was found that PKA inhibition prevented PE-induced increase in Brd4 occupancy <sup>119</sup>. In conclusion, our lab discovered a novel mechanism of G $\alpha$ s-PKA dependent GPCR signaling pathway which is crucial for Brd4 activation in cardiac hypertrophy (**Figure 1.7**) <sup>113,119</sup>.

## 1.6. DREADDs: A chemogenetic platform to specifically activate G protein signaling pathways

My project used genetically engineered G protein-coupled receptors (GPCRs), known as Designer Receptors Exclusively Activated by Designer Drugs (DREADDs), to further probe the function of Brd4 downstream of specific GPCRs. DREADDs are modified to be activated by synthetic small molecules, that are physiologically inert (**Figure 1.7A**). These receptors are designed to respond exclusively to these synthetic ligands, rather than their natural endogenous ligands(**Figure 1.8A**). GPCRs are engineered such that they retain most of their native functions while changing only specific properties, such as agonist binding <sup>121,122</sup>. Thus, DREADDs enable the activation of specific GPCRs in a cell-specific or tissue-specific manner, making it possible to investigate various physiological and pathophysiological pathways associated with GPCRs<sup>123</sup>.





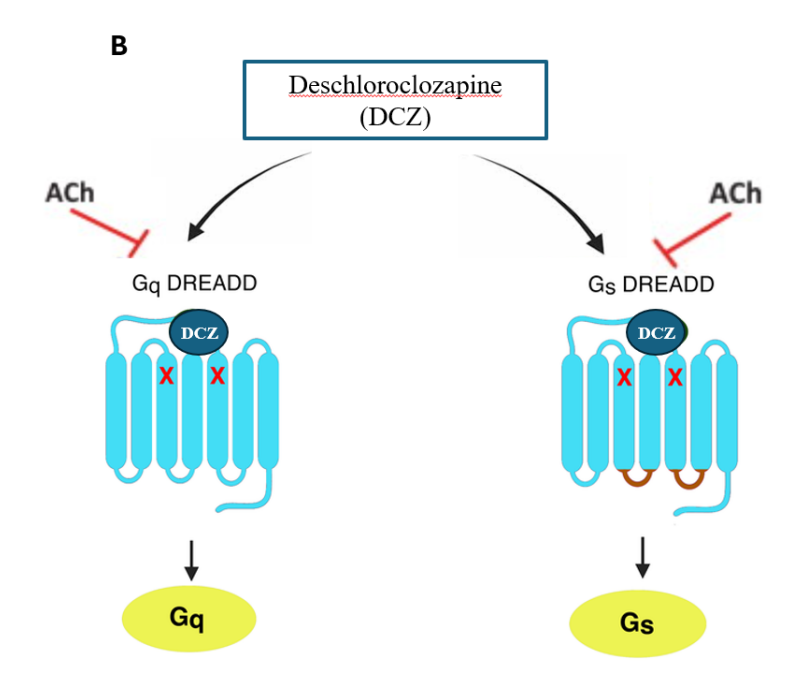


**Figure DREADD** 1.8. Structural and functional **Basis** of Activation DCZ. by (A) Ribbon diagram of the hM3Dq receptor highlighting the structural interactions with the ligands DCZ (magenta) and CNO (gray). The red spheres represent the two key point mutations (Y148C in TM3 and A238G in TM5), which enable specific ligand binding and prevent endogenous muscarinic receptor agonists from activating the engineered receptor. Figure adapted from 123,124. (B) Schematic representation of DCZ's ability to activate both Gq- and Gscoupled DREADDs. The red crosses mark the mutations (Y3.33C and A5.46G) that disrupt binding of endogenous agonists to the modified GPCRs, ensuring selective activation by DCZ. Figure adapted from <sup>125</sup>.

Reprinted by permission from Elsevier publishers, Wess, Jürgen et al." Novel designer receptors to probe GPCR signaling and physiology", Trends in Pharmacological Sciences, Volume 34, Issue 7, 385 – 392 Copyright 2013. Reprinted by permission from Springer Nature publishers, Zhang, S., Gumpper, R.H., Huang, XP. et al. "Molecular basis for selective activation of DREADD-based chemo genetics". Nature **612**, 354–362 Copyright (2022).

The human M<sub>3</sub> muscarinic receptor (hM<sub>3</sub>) based DREADD was one of the first to be established<sup>120</sup>. These muscarinic based DREADDs were developed by introducing two site-specific point mutations Y3.33C and A5.46G. Due to these point mutations, acetylcholine, which is known to be an endogenous agonist of muscarinic receptors was unable to bind to the newly generated DREADD receptors. Instead, it can be activated by a synthetic ligand known as clozapine-N-oxide (CNO) which is known to be high in potency and efficacy<sup>120,123,126</sup>. CNO is known to have high affinity to DREADD receptors but some studies have reported CNO to back-metabolize to clozapine in *in vivo* models<sup>127,128</sup>. Therefore, for my research work, I used

Deschloroclozapine (DCZ) as an agonist, which has been reported to have higher affinity and greater selectivity  $^{129-131}$ .

# Rationale and objectives of this thesis

Brd4 has been implicated in cardiovascular diseases, with our previous work highlighting its recruitment to chromatin during pathological hypertrophy via distinct activation of  $G\alpha$ s and  $G\alpha$ q signaling pathways. GPCRs classically promote cardiac hypertrophy through  $G\alpha$ q signaling, our previous work uncovered that  $\alpha_1$ -adrenergic receptors can also initiate hypertrophic responses through a  $G\alpha$ s-dependent cAMP/PKA pathway. This  $G\alpha$ s-dependent pathway was found to be strongly linked to Brd4, suggesting a general role of this pathway in Brd4 activation. The goal of this thesis was to dissect distinct GPCR-dependent pathways involved in Brd4 activation since it remains unclear how Brd4-dependent transcriptional responses are regulated. This leads me to hypothesize that  $G\alpha$ s and  $G\alpha$ q signaling pathways differentially activate Brd4-mediated gene expression. To explore this, we activated specific G protein signaling pathways using  $G\alpha$ s-coupled and  $G\alpha$ q-coupled DREADDs which were activated using DCZ in transfected HEK293 cells. Our objective was to measure the Brd4-mediated gene expression downstream of  $G\alpha$ s and  $G\alpha$ q signaling pathways. To achieve this, we employed BET inhibitors, JQ1 and dBET6, in conjunction with DCZ to identify changes in gene expression that were induced by G protein signaling and dependent on Brd4 or other BET proteins.

#### MATERIALS AND METHODS

## 2.1 Drugs

# 2.1.1 Drug sources and stock concentrations

BET inhibitors, JQ1 and dBET6 were used to inhibit Brd4. JQ1 (Abcam, ab141498-1MG) and dBET6 (Sigma-Aldrich, SML2683-1MG,) were dissolved in dimethyl sulfoxide (DMSO, Sigma, D2650). Deschloroclozapine (DCZ) was used to stimulate Gαs-coupled and Gαq-coupled DREADD receptors. DCZ (Hellobio, HB9126) was dissolved in sterile water. The drugs were stored in -20°.

# 2.1.2 Drug dilutions

For DCZ, serial dilutions were performed to obtain a range of log dose concentrations. 10mM stock of DCZ was diluted 1:10,000 in sterile water to bring the concentration to 1µM. This dose was used to obtain 6 log dose concentrations. For JQ1, 1mg of JQ1 was diluted in 433.37µl DMSO to obtain a concentration of 5mM. This was further diluted to its final concentration as mentioned in **Table 1**. For dBET6, 1mg of dBET6 was diluted in 2.37ml DMSO to obtain a concentration of 500uM. This was further diluted to its final concentration as mentioned in **Table 1** below.

Table 1: Drug concentration and dilution.

Drug	Stock	Dilution	Final conc.
Conditions	Conc.		
JQ1	5mM	2μl stock + 8μl media = 1mM	$1:1000 = 1 \mu M$
dBET6	500μΜ	$2\mu$ l stock + $8\mu$ l media = $100\mu$ M	1:1000 = 100nM

#### 2.2 Plasmids

The plasmids, pcDNA5/FRT-HA-hM3D (Gq) and pcDNA5/FRT-HA-rM3D (Gs) were obtained from Addgene (plasmid # 45547; http://n2t.net/addgene:45547; RRID:Addgene\_45547; plasmid # 45549; http://n2t.net/addgene:45549; RRID:Addgene\_45549) 132. To check the purity

of these plasmids, 1% agarose gel electrophoresis was performed. To digest the plasmid, BamHI and Not1 restriction enzymes (New England Biolabs, cat#R3136, cat#R3189) were used. For restriction enzyme digestion, the reaction set-up consisted of 2µg of DNA, 4.2µl of 10X rCutSmart Buffer (New England Biolabs, cat#B6004) and 1µl of the restriction enzyme. The volume was adjusted to 50µl using nuclease-free water. It was incubated overnight at 37°C. After adding 4µl of loading dye, the samples were loaded on a 1% agarose gel (refer to supplementary **Figure S1**).

# 2.3 Cell culture and transfection

HEK 293 parental (PL) cells were maintained in Dulbecco's Modified Eagle's medium (DMEM) high glucose + 5% (v/v) fetal bovine serum + 1% (v/v) penicillin/streptomycin. HEK 293 PL cells were incubated at 37°C.

For BRET assays, the cells were cultured in Dulbecco's Modified Eagle Medium (DMEM; Multicell 319-015-CL), supplemented with fetal bovine serum (FBS; Wisent 095-150) and penicillin-streptomycin (P/S; Wisent 450-201-EL). Cells were passaged in T75 flasks (Thermo Scientific 130190) and 6-well plates (Corning 3516). For cell detachment, 0.25% trypsin-EDTA (Wisent 325-043-CL) was used. Cells were transfected with Lipofectamine 2000 (Invitrogen 11668030) according to the manufacturer's instructions 24h after plating. On day 1, 250,000 cells were seeded on 6 well plates. On day 2, transfections were performed in DMEM HG + 2.5% FBS (without P/S) media. A total of 1 µg of the respective biosensor DNA and 0.5 µg of the receptor DNA were used for transfection. For each well, 1 µg of the respective biosensor DNA and 0.5 µg of the receptor DNA was transfected. For each control, 0.5 µg of pcDNA3.1(-) and 1 µg of EPAC biosensor 133 or PKC biosensor 134 was added to each well in a 6-well plate. For each DREADD receptor, 0.5µg of Gas-DREADD/Gaq-DREADD and 0.5µg of their respective EPAC/PKC receptor was added to each well in a 6-well plate. After 4-5 hr. incubation, the media was replaced with DMEM HG media + 5% FBS + P/S. On day 3, cells were detached with 0.25% trypsin-EDTA (Wisent) and plated at a density of 30,000 cells/well in a poly-L-ornithine hydrobromide solution (Sigma-Aldrich, P3655-100MG)-coated 96-well white bottom plate (Thermo Scientific, 236105) for BRET. Cells were incubated for another 24h prior to biosensor experiments. On the day of the experiment i.e., day 4, cells were starved in Kreb's buffer (146 mM NaCl, 42 mM MgCl<sub>2</sub>, 10 mM HEPES pH 7.4, 1g/L D-glucose) prior to imaging assays, and the same buffer was used to dilute

the drug stock solutions. DMEM media was aspirated, and 150 ml of Krebs buffer was added and then aspirated again. Following this, 80ul of Krebs buffer was added to each well and incubated in a parafilm wrapped 96-well plate.

For protein extraction, on day 1, 350,000 cells were seeded in each well of a 6-well plate. On day 2, each well was treated with 100nM dBET6 for a different time and cells were harvested for protein extraction.

For RNA analyses, 350,000 cells/well were seeded in a 6-well plate for each treatment. On day 2, cells were transfected using Lipofectamine 2000 according to the manufacturer's instructions 24h after plating in 2.5% FBS DMEM HG media (without P/S). For each DREADD receptor, 0.5μg of Gαs-DREADD/Gαq-DREADD and 0.5μg of their respective EPAC<sup>133</sup>/PKC<sup>134</sup> receptor was added to each well in a 6-well plate. After 4-5 hr. incubation, the media was replaced with DMEM HG + 5% FBS + P/S. On day 3, drug treatments were performed. JQ1 (1uM) and dBET6 (100nM) were treated for 3hrs and DCZ (1uM) for 1hr. The cell lysates after drug treatment were obtained using the TRI reagent® RNA Isolation Reagent (Sigma, T9424).

#### 2.4 BRET measurements

A TriStar 2 Multimode Plate Reader (Berthold Technologies) was used for a 5-minute basal reading. The temperature within the plate reader was maintained at 28°C and the set for BRET-2 with a 380-650 nm spectral range using the 'ICE' software package (Berthold Technologies). After one-hour incubation of the 96-well plate, 10μl of Coelenterazine 400A (Cedarlane) was added (final dilution of 1:500) to each well. After adding this substrate, we wait for 5 mins and then record the BRET readings. These readings were taken by placing the plate in TriStar 2 Multimode Plate Reader and using the 'ICE' software package (Berthold Technologies), a temperature of 28°C was maintained and the filters were adjusted to 410-515 nm spectral range. After the basal reading, the vehicle was added to the first well, while DCZ was added at six different concentrations (as mentioned in section 1.2), spanning 6-log dose responses. The drugs were added at a 1:10 dilution (i.e., 10μl added to 90μl) to each well. The measurements were taken at three time points: 10 mins, 20 mins and 30 mins.

### 2.5 BRET analysis

BRET ratios were calculated at 515/410 nm emission which was calculated by dividing the acceptor fluorescence by the donor luminescence (acceptor/donor). Further,  $\Delta$ BRET was calculated i.e., (Stimulated agonist BRET ratio – basal agonist BRET ratio) – (Stimulated vehicle BRET ratio – Vehicle BRET ratio). In this case, DCZ was the drug which stimulated the Gascoupled and Gaq-coupled DREADD receptors. The following equations used for both Gas and Gaq-DREADD receptors, for which EPAC and PKC biosensors were used, respectively:

 $\triangle BRET_{G\alpha s} = [(G\alpha s - DREADD - EPAC/DCZ) - (G\alpha s - DREADD - EPAC)] - [(pcDNA - EPAC/DCZ) - (pcDNA - EPAC)].$ 

 $\Delta BRET_{G\alpha q} = [(G\alpha q - DREADD - PKC/DCZ) - (G\alpha q - DREADD - PKC)] - [(pcDNA - PKC/DCZ) - (pcDNA - PKC)].$ 

An average of three technical replicates were considered for all these calculations. Graphs were made using GraphPad Prism 10.0 for each time point, where y-axis represented  $\Delta$ BRET and x-axis represented the log dose concentrations of DCZ.

#### 2.6 Protein extraction and Western blot

Cells in each well were washed using cold PBS twice and then were lysed using RIPA buffer (1% NP-40, 50 mM Tris-HCl pH 7.4, 150 mM NaCl, 1 mM EDTA, 1 mM EGTA, 0.1% SDS, 0.5% sodium deoxycholate). Approximately, 200-400µl cold RIPA was added to each well. The 6-well plates were kept on ice for 10 mins. Using a cell scraper, cells were scraped and then transferred to a labelled Eppendorf on ice. This cell suspension was mixed (approx. 20 times) using a syringe/pipette to form a homogenous mixture. Then cell lysates were incubated on ice for 15 mins. Samples were then spun in a microcentrifuge (Eppendorf, Centrifuge 5425/5425R) at 14,000 x g for 15 mins at 4°C. The supernatant was transferred to a new Eppendorf and then protein was quantified by BCA (Bicinchoninic acid) assay. For BCA, a fluorescence-based PierceTM BCA kit (Thermo Scientific, 23225) was used as per manufacturer instructions.

Western blot was done to optimize the RNA seq conditions for dBET6 inhibitor in HEK293 cells. Protein samples were denatured at 95°C for 2 to 5 mins in 4X Laemmli buffer supplemented with 5% β-mercaptoethanol. For SDS-page, protein lysates were loaded on 8% Tris-glycine gel and were run on Bio-Rad Protean ® electrophoresis unit (Bio-Rad, 525BR). The electrophoresis apparatus was set up at 120V for 15 mins and then at 170 V for 45 mins in running buffer (3.02g Tris, 18.8g glycine, 10ml of 10% SDS dissolved in 700 ml ddH<sub>2</sub>O). The protein was transferred onto a nitrocellulose membrane (Bio-Rad, 1620115), in cold transfer buffer (3.63 g Tris, 15 g Glycine, 0.5g SDS dissolved in 800 mL ddH2O, 200ml 100% MeOH) at 200mA for an hour using a stirring bar in Bio-Rad Protean® Transfer Tank. Blocking of the membrane was performed with 5% skim milk (20ml/membrane) diluted in TBST (8.78g NaCl, 10mL 1M Tris pH 8.0, 0.5 mL Tween-20 dissolved in 1L ddH<sub>2</sub>O) for an hour. Following this, western blots were probed with primary antibody i.e., Brd4 antibody (Invitrogen, PA585662; 1:2000) in 5% skim milk overnight at 4°C. The next day, membranes are washed thrice for 5 mins each with 10ml TBST per membrane shaking at room temperature. The nitrocellulose membranes were then probed with secondary HRP-mouse antibody at 1/5000 (vwr, CA95017-332L) in blocking solution (5% skim milk in TBST) shaking at room temperature for an hour. For control, β-tubulin (Invitrogen, 32-2600) or GAPDH (Invitrogen, AM-4300) were used at a concentration of 1:500. The blots were treated with GE ECL Select (GE, RPN2235) and were developed using GE Amersham Imager 600. Western blot images were quantified using ImageJ.

### 2.7 RT-qPCR

After the drug treatment, the cells were detached from the 6-well plate using the TRI reagent. Using a cell scraper, the cells were removed from the wells and transferred to an Eppendorf. Bromo-chloro-propane (BCP) is added to these cell suspensions after which there were vortexed and incubated for 15 mins at room temperature, following which they were centrifuged at 12,000 rpm for 15 mins at 4°C. BCP causes phase separation, and the aqueous supernatant containing the RNA was transferred to a new Eppendorf tube. To this, an equal ratio of isopropanol was added to the supernatant. Further, the samples were centrifuged at 12,000 rpm for 8 mins. The pellet was washed with 70% ethanol and resuspended in RNAase free H<sub>2</sub>O. The RNA isolated was

quantified using Nanodrop spectrophotometer (Thermo Fisher). RNA samples were quantified using Nanodrop. cDNA synthesis was primed with random hexamers (IDT, 51-01-18-01) using M-MLV reverse transcriptase. For qPCR, cDNA was diluted to a concentration of 5  $\mu$ g/ $\mu$ l and stored at -20°C. A 1:10 dilution of the cDNA was prepared. In a 96-well plate, 90ul H<sub>2</sub>O, 10  $\mu$ l of diluted cDNA, and BrightGreen 2X qPCR Mastermix were added using a micropipette. The plate was then spun using a plate microcentrifuge to collect all the reagents at the bottom of each well. qPCR was performed using a ViiA 7 Real-Time PCR System (Thermo Scientific). The PCR results were analyzed via the 2-ddCt method. An average of three readings were taken and were normalized to GAPDH (housekeeping) and DMSO. Then we exponentiated the normalized values by the power of 2 to calculate the fold change. The primer sequences for c-myc were designed using NCBI primer BLAST. The following were the sequences for c-myc:

Forward primer (5' GCCGCATCCACGAAACTTT 3')
Reverse primer (5' TCCTTGCTCGGGTGTTGTAAG 3')

### 2.8 RNA isolation for RNA sequencing

For RNA seq analysis, the RNEasy Mini kit (Qiagen, 74104) and Qiashredder Homogenization kit (Qiagen, 79645) were used as per manufacturer instructions. RNA seq samples were quantified using a Nanodrop spectrophotometer. The collected cDNA was placed in a 0.5 mL microtube. From the total cDNA, 100 µL at a concentration of 100 ng/µL was transferred to 1.5 ml Eppendorf tube. A total of 24 samples (12 X 2) were sent for RNA sequencing. PolyA enriched RNA library preparation, Illumina library QC and Illumina NovaSeq PE100 -25M reads were performed by Genome Québec.

### 2.9 RNA seq analysis

FASTQ files were obtained which were subjected to adaptor trimming and FASTP (v0.23.4) was used to filter the low quality and duplicate files<sup>135</sup>. Following this the sequences were aligned to Homo sapiens genome (GRCh38, NCBI # GCF\_000001405.26) using STAR alignment (v2.7.11b)<sup>136</sup>. Using FeatureCounts (v2.0.1) individual matrices were obtained. All the bash commands were written in Python and were summarized into a text file for further analysis on R (v.4.3.2).<sup>137,138</sup> The FeatureCounts files obtained were normalized to the control group (i.e.,

DMSO+Gas for Gas-DREADD and DMSO+Gaq for Gaq-DREADD group of treatments). Differential expression analysis was performed. DESeq2 (v1.42.1) package was installed. According to the treatments, two DESEQDataSet (dds) objects were created. <sup>139</sup> The gene sets were then segregated into significant upregulated and downregulated genes. Using Venn diagrams the treatments were compared. Volcano plots for each treatment were generated using ggpolot2. GO (gene ontology) enrichment analysis was performed using the EnrichGO function using the clusterProfiler package (v4.10.1)<sup>140</sup>. GO terms were categorized into biological processes (bp), molecular functions (mf), and cellular compartments(cc) which were plotted using dot plots. Dot plots described the KEGG pathways wherein the genes were involved 141,142. The upregulation of genes between different treatments was compared, and the corresponding KEGG pathways were identified to reveal functional insights. For the significant genes, Bulk Transcription Factor Interference was calculated using the decoupleR (v 2.10.0) package, enabling a detailed analysis of transcription factor activities across the treatments <sup>143</sup>. The results include an in-depth description of these analyses, covering a wide spectrum of treatment conditions and their impact on gene expression. A thorough examination of the experimental procedures and the subsequent data analysis is presented in the next section.

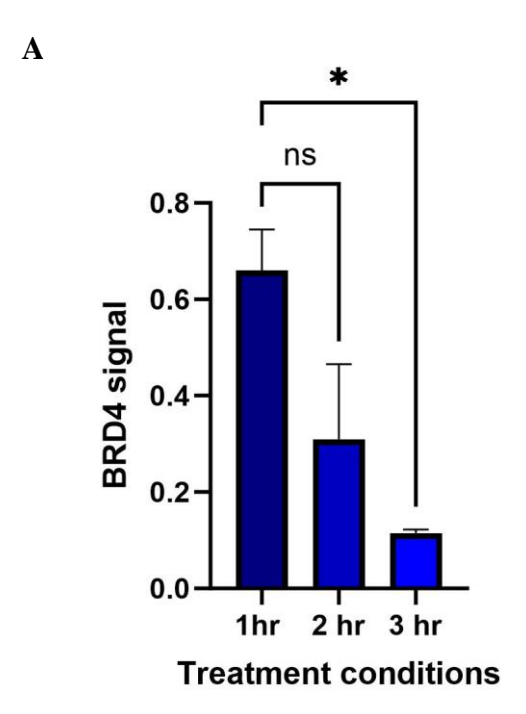
#### RESULTS

### 3.1 Optimization of BET inhibitor treatment conditions

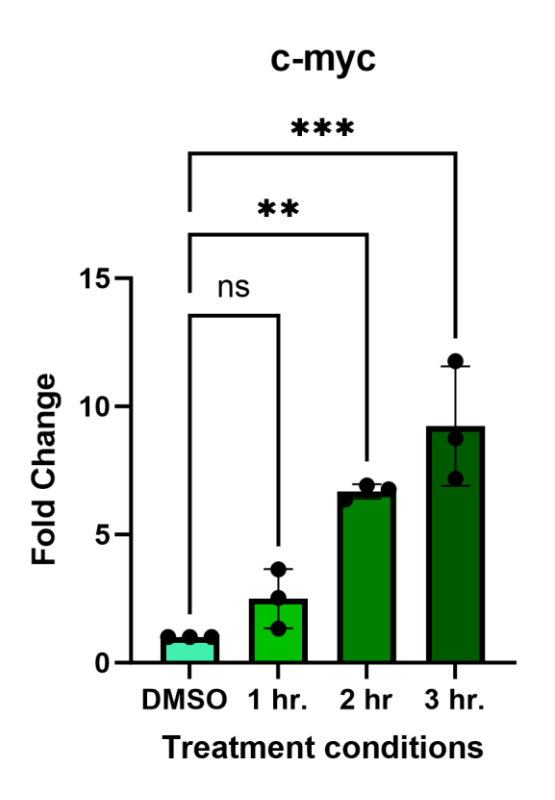
BET inhibitors were optimized for use in HEK293 cells by treating for 1 hr., 2 hr., and 3 hr. time points. For dBET6, we evaluated the effective dose based on a previous study <sup>144</sup>. The study concluded that a 100nM dose of dBET6 is effective based on its ability to disrupt expression of genes such as c-myc <sup>144</sup>. We further evaluated dBET6 (100nM) at three different timepoints using western blot analysis of Brd4 levels (**Figure S2**) and quantified using ImageJ, as depicted in **Figure 3.1A**. The effect of dBET6 was found to be time dependent as the effect was found to be the least at 1 hr. time point. dBET6 treatment at 3 hrs. was found to be the most effective time point.

Based on our understanding of P-TEFb regulation, we optimized JQ1 treatment with a focus on c-myc levels. Previous studies have shown that BET inhibitors like JQ1 reduce c-myc expression and Myc-dependent gene expression 105,144,145. However, we observed an unexpected increase in c-myc levels (**Figure 3.1B**), suggesting a potential disruption in the P-TEFb balance within cells. JQ1 treatment displaces P-TEFb from the 7SK snRNP complex and Brd4 from chromatin, leading to an accumulation of free P-TEFb, which acts as a transcriptional activator to promote elongation of target genes, including c-myc. Studies have also shown that JQ1 increases the association of P-TEFb with Brd4<sup>146-149</sup>. Based on this, we used c-myc as a parameter to optimize JQ1 efficacy. While a 1-hour treatment showed no significant effect, we observed that JQ1's effectiveness is time-dependent, with 2- and 3-hour treatments significantly upregulating c-myc levels. Notably, JQ1 was most effective at the 3-hour mark. Additionally, we performed a combined treatment of JQ1 with DCZ to assess whether DCZ interferes with the effects of JQ1 (**Figure S4**). Together, these findings indicate that both BET inhibitors, JQ1 and dBET6, were maximally effective at 3 hours.

Figure 3.1.



B



3.1. Western blot and RT-qPCR analysis to confirm effects of BET inhibitors (A) shows the protein expression of Brd4 upon the treatment with dBET6 using anti-Brd4 which was quantified using ImageJ (bars = Mean +/- SEM of n=2; biological replicates).  $\beta$ -tubulin were used to normalize the protein expression. This was done at three different time points: 1hr, 2hr and 3hr. One-way ANOVA was performed followed by Dunnet's *post hoc* test \*p < 0.1 (B) RT-qPCR was done to measure c-myc levels upon treatment with JQ1. It was done at three different time points: 1hr., 2 hr. and 3 hr. One-way ANOVA was performed followed by Dunnet's *post hoc* test \*\*\*p < 0.001, \*\*p < 0.1. (biological replicates n=3)

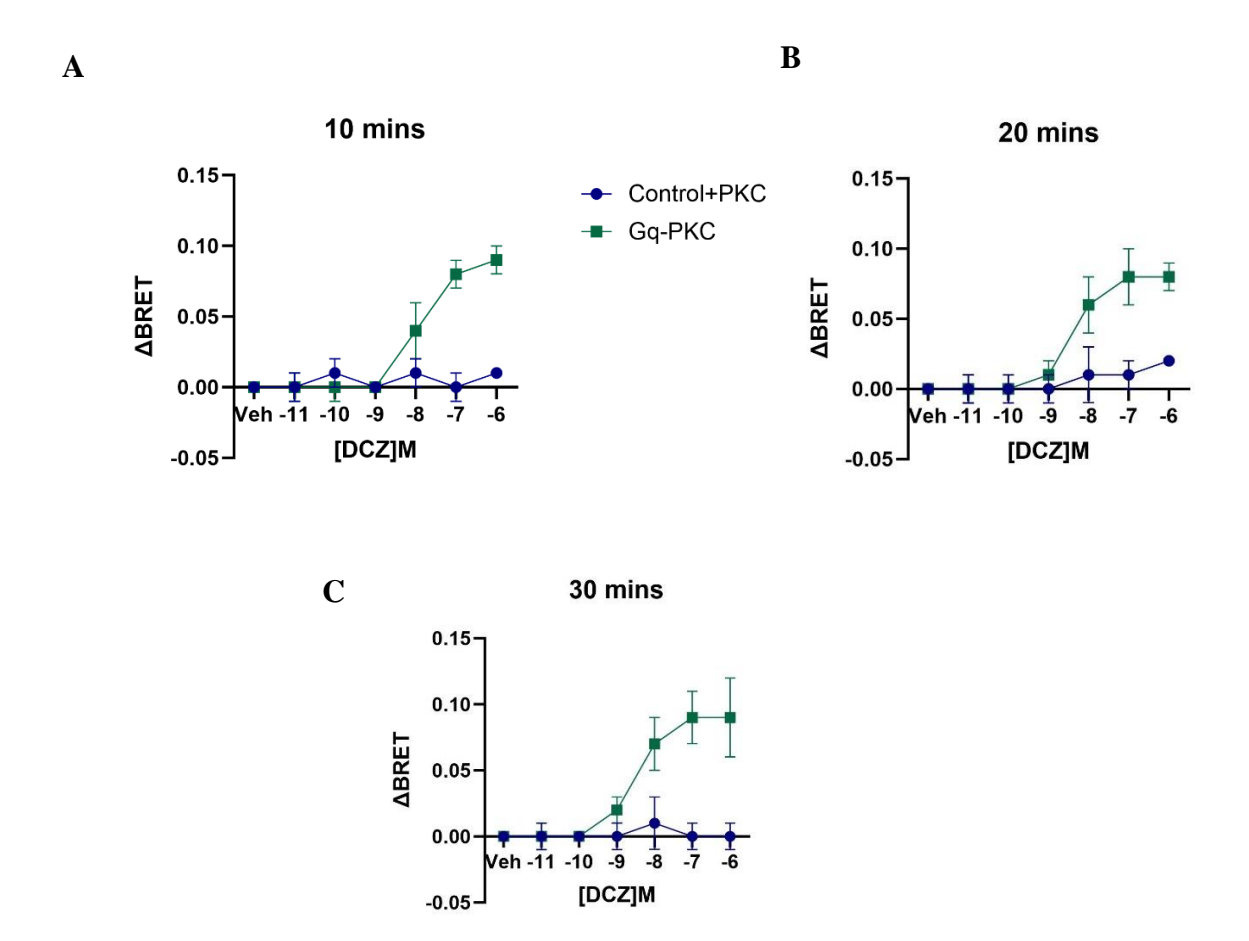
### 3.2. Activation of Gas-coupled and Gaq-coupled DREADD receptors using DCZ.

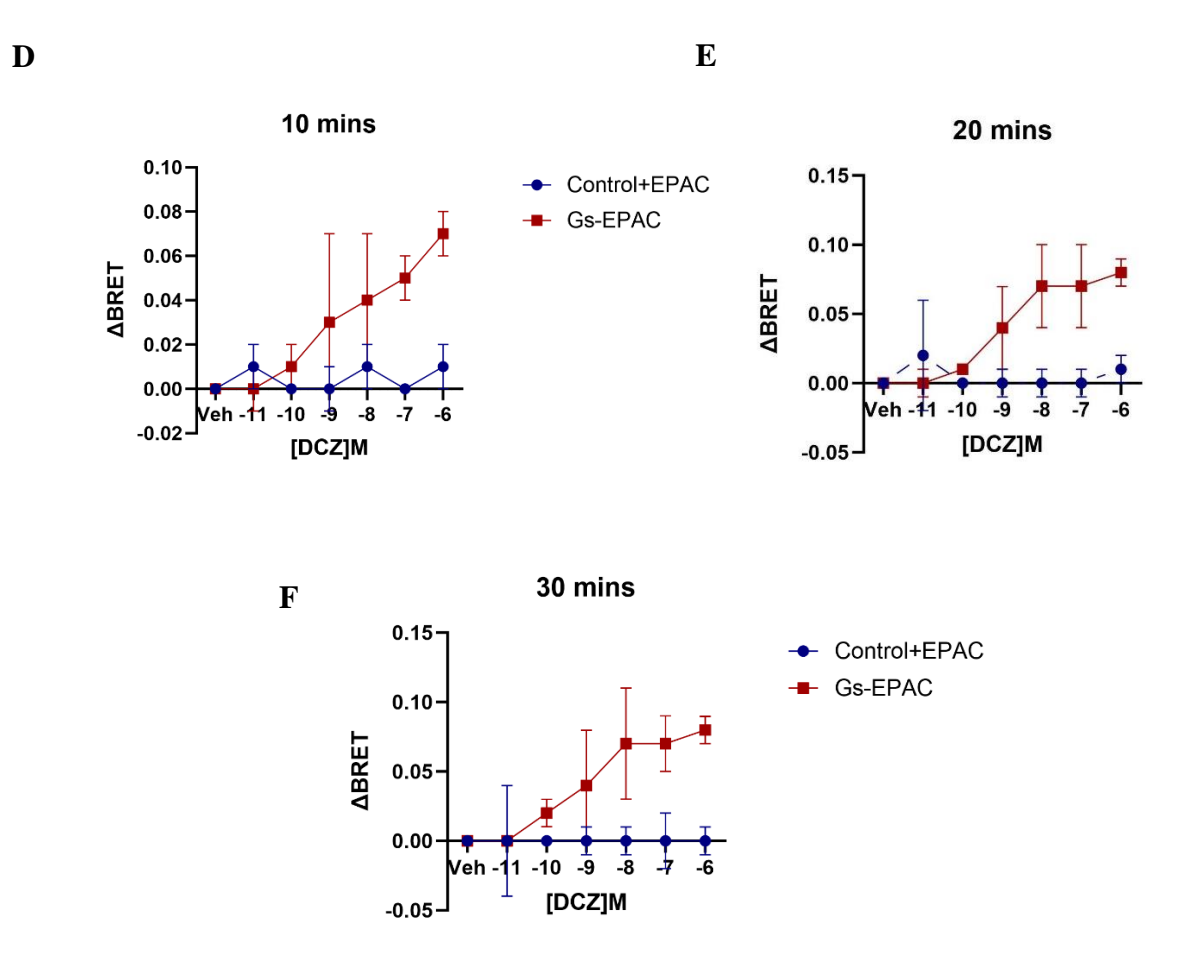
To optimize DCZ concentrations at different time points and to ensure if the system works well in activating G $\alpha$ s- and G $\alpha$ q-DREADDs, BRET analysis was done using (BRET)-based EPAC and PKC biosensors <sup>134,150</sup>. A series of log dose concentrations of DCZ (from  $10^{-6}$  to  $10^{-11}$ ) was accessed. BRET analysis is shown in **Figure 3.2**.  $\Delta$ BRET is measured against the DCZ concentration plotted in the log scale. Data observed in **Figure 3.2** represents G $\alpha$ q-DREADD coexpressed with a PKC biosensor. The data were collected at different time points: 10 mins, 20 mins, and 30 mins. At 10 mins, DCZ starts showing its effect from  $10^{-8}$  M, with a strong response at  $10^{-7}$  M and  $10^{-6}$  M. The G $\alpha$ q-PKC group showed a significant increase in  $\Delta$ BRET compared to the control group, especially at higher DCZ concentrations (**Figure 3.2A**). At 20 mins, the trend observed at 10 min continues, with further increases in  $\Delta$ BRET in the G $\alpha$ q-PKC group as DCZ concentrations increase, but the magnitude of response is slightly reduced compared to the 10 min point (**Figure 3.2B**). At 30 mins, the G $\alpha$ q-PKC response begins to plateau, and the  $\Delta$ BRET values are consistent but do not increase much beyond the earlier time points (**Figure 3.2C**).

Similarly, data was collected for the G $\alpha$ s-DREADD using an EPAC biosensor. The data again represents different time points: 10 mins, 20 mins, and 30 mins. DCZ again shows an uptick at 10 mins suggesting an effective response, with G $\alpha$ s-EPAC activation becoming prominent at concentrations of  $10^{-7}$  M and  $10^{-6}$  M. The effect was found to be more significant compared to the control group at this time point (**Figure 3.2D**). Similar to G $\alpha$ q-PKC, at 20 mins, G $\alpha$ s-EPAC shows continued activation at higher concentrations, but the  $\Delta$ BRET increase is reduced compared to 10 mins (**Figure 3.2E**). Again, the response plateaus at 30 mins, with a consistent  $\Delta$ BRET that remains higher than control but without a significant increase beyond 10 mins (**Figure 3.2F**). Therefore, DCZ at 1  $\mu$ M ( $10^{-6}$  M) was found to be the most effective concentration at activating both G $\alpha$ s and G $\alpha$ q-DREADDs, with the peak effect observed at the 10-minute time point.

Together, The BRET-based analysis with PKC and EPAC biosensors successfully demonstrated that the system works well with DCZ activating the DREADDs. The data show consistency in the effective responses as can be seen from the analysis. The results confirm that 10 mins treatment with 1  $\mu$ M DCZ is optimal for G protein activation in this system.

Figure 3.2.



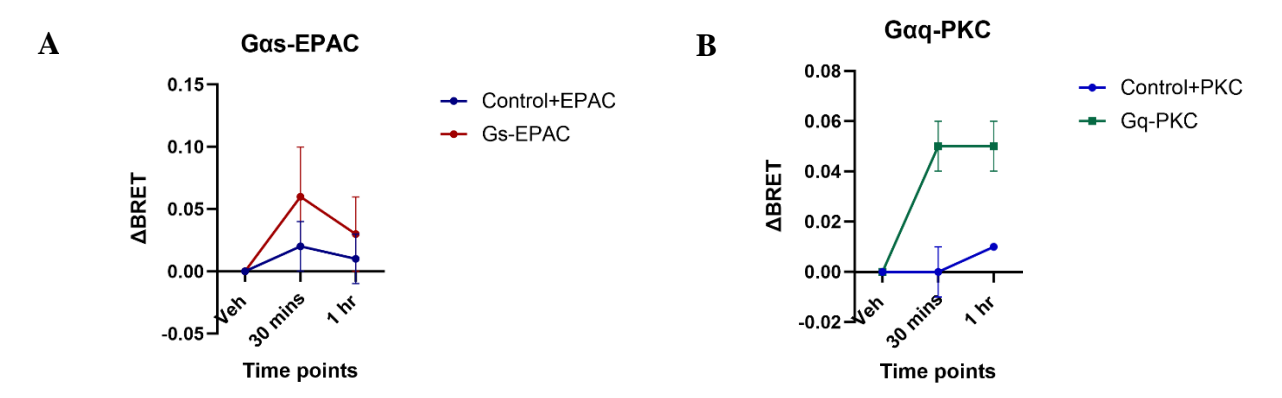


3.2. BRET analysis of G $\alpha$ q-DREADD and G $\alpha$ s-DREADD activated using DCZ. (A-C) represents the  $\Delta$ BRET of G $\alpha$ q-DREADD and (B-F) G $\alpha$ s-DREADD activated by DCZ from 10<sup>-6</sup> to 10<sup>-11</sup> log dose concentrations at 10-, 20- and 30-min time points (biological replicates n=3).

Next, to optimize the DCZ receptor activation for RNA sequencing, we wanted to try longer time points with the same dose. Thus, we examined receptor activation at 1 hour time point with DCZ ( $1\mu M$ ) for both the receptors (**Figure 3.3A & B**). The BRET data indicates that DCZ still activates the receptor under these conditions. For Gas-EPAC, receptor activation is transient, peaking at 30 minutes and returning to a lower activation level after 1 hour. The 1-hour time point was selected to capture active signaling, thereby optimizing conditions to identify differentially expressed genes (**Figure 3.3A**). However, for Gaq-PKC, receptor activation is sustained even after 1 hour, suggesting a prolonged response (**Figure 3.3B**). Thus, the BRET analysis suggests that DCZ activates the receptor, especially in the sustained PKC activation pathway, leading us to use this time point for our RNA-seq experiments.

.

Figure 3.3.



3.3. BRET analysis of DCZ activation at longer time points. (A) represents the  $\triangle$ BRET of G $\alpha$ q-DREADD and (B) G $\alpha$ s-DREADD activated by DCZ at 10<sup>-6</sup> (1 $\mu$ M) at 30-min and 1 hour time points (biological replicates n=3).

# 3.3 Transcriptomic Profiling of Gaq and Gas modulation in response to JQ1 and dBET6 Treatments via RNA Sequencing

To investigate the differential gene expression associated with G $\alpha$ q and G $\alpha$ s DREADD receptors, we tested several RNA-seq conditions. The control condition used G $\alpha$ q/G $\alpha$ s-DREADD with DMSO. To analyze gene expression changes upon receptor activation, we treated G $\alpha$ q/G $\alpha$ s-DREADD with the agonist DCZ. Additionally, BET inhibitors dBET6 and JQ1 were tested with and without receptor activation to examine the impact of these inhibitors in modulating gene expression in the presence of receptor signaling. **Table 2** depicts the specific conditions for each receptor.

Table 2:

DREADDs	Treatment conditions
	DMSO + Gαq-DREADD
	DCZ + Gαq-DREADD
Gαq	JQ1 + Gαq-DREADD
	dBET6 + Gαq-DREADD
	$JQ1(3hr) + DCZ(1hr) + G\alpha q - DREADD$
	dBET6 (3hr) + DCZ (1hr) + Gαq-DREADD

Gαs	DMSO + Gαq-DREADD
	DCZ + Gαq-DREADD
	JQ1 + Gαq-DREADD
	dBET6 + Gαq-DREADD
	$JQ1(3hr) + DCZ(1hr) + G\alpha q$ -DREADD
	$dBET6 (3hr) + DCZ (1hr) + G\alpha q-DREADD$

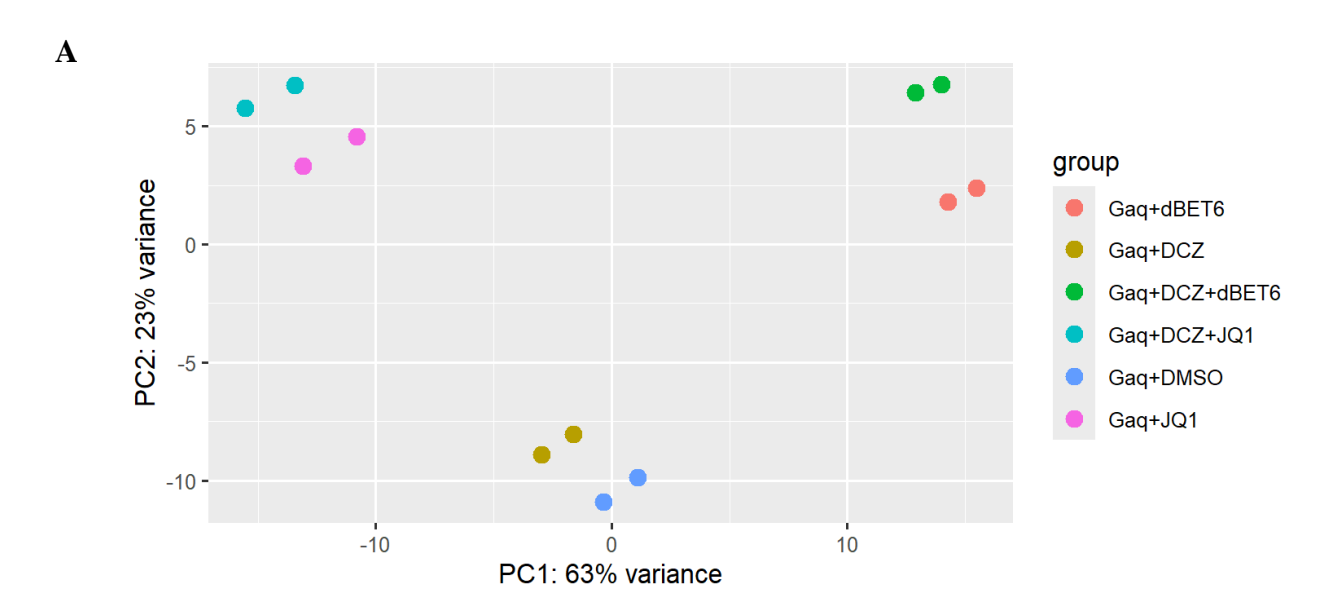
Table 2: Treatment conditions for Gaq and Gas-coupled DREADD receptors for RNA seq. The treatment conditions include DMSO as a control.  $1 \mu M$  DCZ was the agonist treated for an hour, used to activate the receptor. BET inhibitors, JQ1 and dBET6 were treated for 3 hrs. A total of 24 samples were sent for sequencing (n=2).

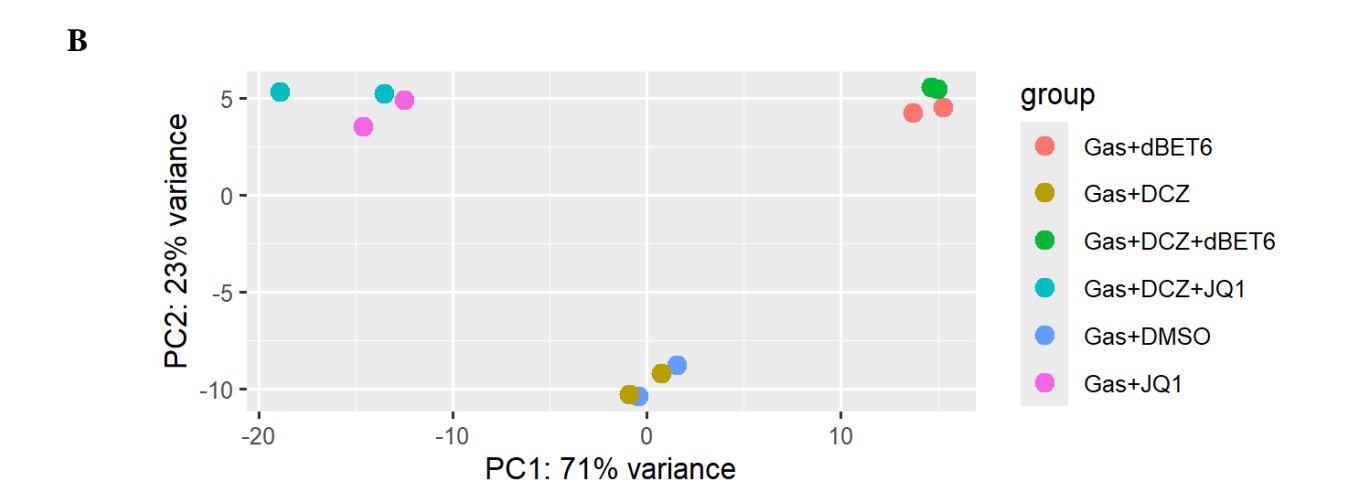
First, we looked at the clustering of various treatment conditions and their replicates based on their transcriptomic profiles using PCA plots. **Figure 3.4A&B** represents Gαs and Gαq activation conditions. They indicate strong consistency in the data, confirming that the experimental replicates produce similar gene expression profiles. In both figures, we considered the Gαs/Gαq + DMSO to be the control condition. In both cases, there is a clear separation between the profiles of dBET6 treatments and JQ1 treatments which indicates that these two inhibitors induce distinct transcriptomic changes, affecting different molecular pathways or having unique impacts on gene expression. Both BET inhibitors, JQ1 and dBET6, show a clear and substantial separation from the untreated condition (DMSO) in the PCA plots (Figure 3.4 A&B), indicating that they induce much more pronounced transcriptomic changes. In contrast, the DCZ treatment group is clustered closer to the untreated control (DMSO), suggesting that DCZ causes relatively smaller changes in gene expression. This distinct clustering of JQ1 and dBET6 away from both DCZ and untreated samples highlights the strong impact of BET inhibitors on gene expression, suggesting they alter cellular transcriptional programs more significantly than DCZ.

The  $G\alpha q + JQ1/dBET6 + DCZ$  treatment points are positioned at a considerable distance from their respective non-DCZ treatments, suggesting a substantial change in transcriptomic response upon receptor activation by DCZ (**Figure 3.4A**). In contrast, the  $G\alpha$ s activation shows a tighter clustering between inhibitor + receptor activation and inhibitor-only conditions, indicating a less robust transcriptomic shift with  $G\alpha$ s activation (**Figure 3.4B**). Further analysis of the activated genes in these conditions will provide clearer insights into the specific pathways modulated by

Gas. For Gaq, the separation between inhibitor-only and inhibitor+receptor treatments strongly suggest an altered transcriptomic response compared to Gaq activation alone.

Figure 3.4.





3.4. PCA plot for transcriptomic profiling of all the treatments. The PCA plots illustrate the clustering of various treatment conditions for (A)  $G\alpha q$  and (B)  $G\alpha s$  receptors based on their transcriptomic profiles, with each point representing a replicate. The x-axis (PC1) and y-axis (PC2) capture the majority of variance in the data, with 63% and 71% variance for  $G\alpha q$  and  $G\alpha s$ , respectively. Each treatment condition is color-coded, with DMSO as the control (blue), JQ1 alone (magenta), DCZ alone (olive), and BET inhibitors dBET6 or JQ1 combined with DCZ (cyan and

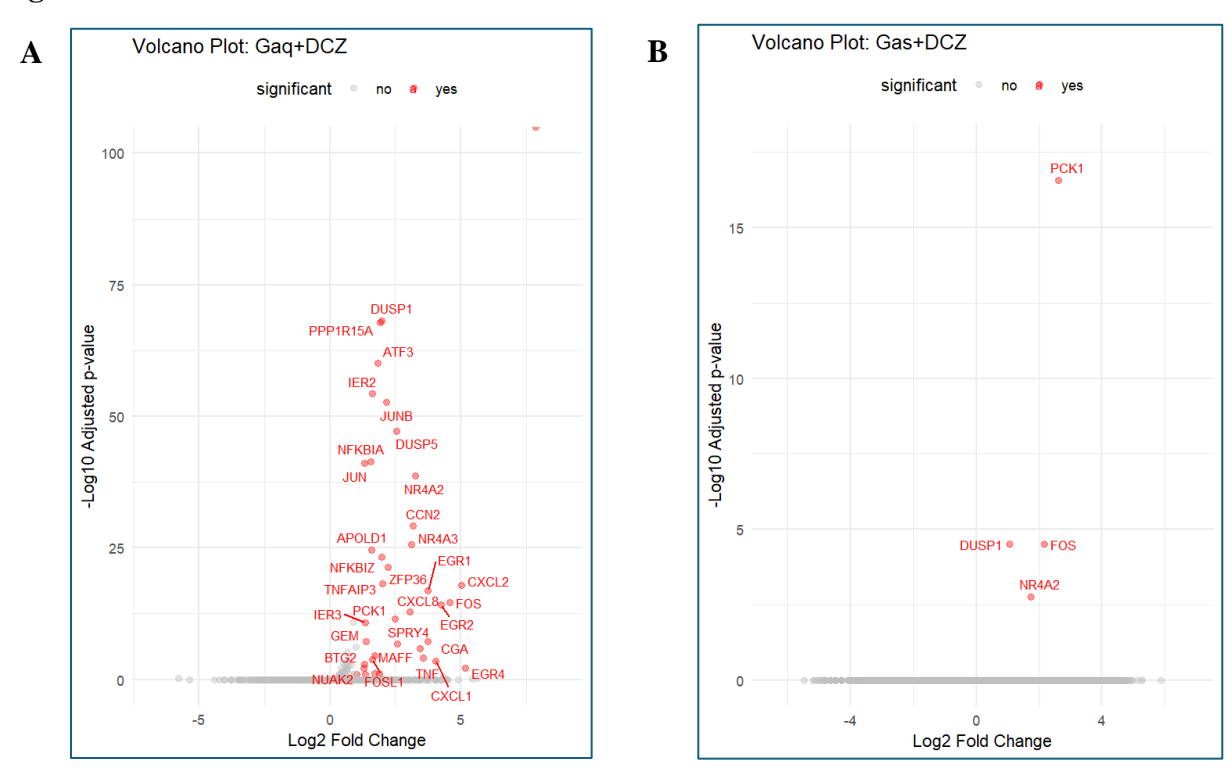
green, respectively). The control group serves as a baseline for comparison. Overall, the PCA plots confirm the consistency of replicates and highlight differential transcriptomic responses to treatments across conditions.

# 3.4. Transcriptomic analysis of the effect of BET inhibitors on $G\alpha$ s and $G\alpha$ q-mediated gene expression

First, we begin with the analysis of  $G\alpha q$  activation. We used volcano plots to show effects on gene expression. Differentially expressed genes were obtained using the adjusted p values of the DEseq2 results. The adjusted p value cutoff was set to 0.1 and we filtered the genes based on the absolute log2 fold change of more than 0.58 (corresponding to a fold-change cutoff of 1.5-fold). The upregulated and downregulated genes can be seen within the volcano plots generated for the treatments.

The plot represents the treatment of  $G\alpha q+DCZ$  normalized to  $G\alpha q+DMSO$  (**Figure 3.5A**). Log fold change is plotted against log adjusted p-values. As observed from the plot, the values of the genes shown in red are the significant genes passing the cutoff criteria. These genes can also be seen in the right quadrant of the plot signifying a positive log fold change or genes which were found to be upregulated. The total number of genes activated were 55 in the case of  $G\alpha q$ . Significant genes, marked in red, include several highly upregulated ones like *DUSP1*, *ATF3*, *IER2*, and *JUNB*, suggesting a strong transcriptional response. Other activated genes, such as *CXCL1* and *EGR4*, appear to be less prominent. Similarly, **Figure 3.5B** shows the genes upregulated by activation of  $G\alpha s$ . However, only four genes were activated by  $G\alpha s$ . These upregulated genes are known to be involved in pathological processes. In the subsequent sections, we will explore the potential significance of these upregulated genes in the context of  $G\alpha s$  activation.

Figure 3.5.



3.5. Volcano plots depict receptor activation. (A) This volcano plot shows gene expression changes after  $G\alpha q + DCZ$  treatment. The x-axis represents log2fold change, and the y-axis indicates -log10 adjusted p-value. (B) This plot shows gene expression changes after  $G\alpha s + DCZ$  treatment. Four genes are significantly upregulated: PCK1, DUSP1, NR4A2, and FOS, with PCK1 showing the most notable increase. Genes upregulated were significant by p adj. < 0.1 and logfc > 1.

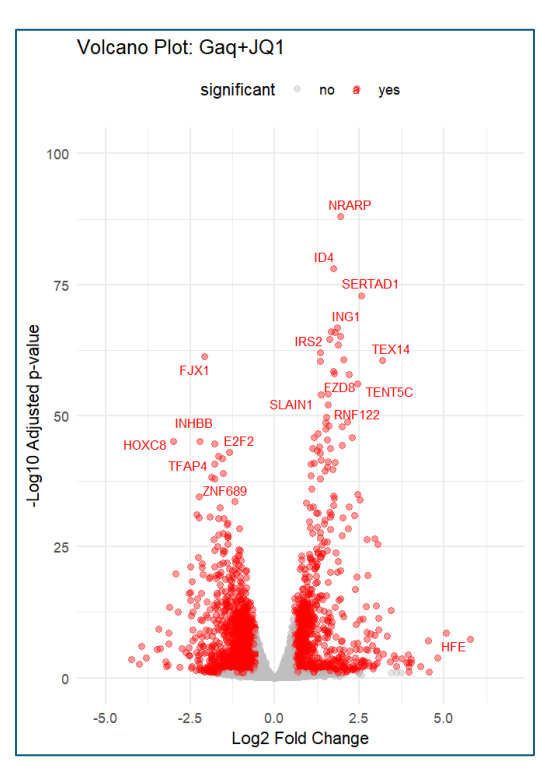
We tested both the BET inhibitors, JQ1 and dBET6 for their effects on gene expression either on their own or in combination with DREADD activation. The volcano plots show that without receptor activation ( $G\alpha q+JQ1$ ), gene expression changes are widespread, with 859 genes significantly up- or downregulated (**Figure 3.6A**). This is consistent with the involvement of BET proteins in transcription of many genes, as has been shown previously <sup>90,151</sup>. With receptor activation ( $G\alpha q+DCZ+JQ1$ ), in **Figure 3.6B**, it was observed to have a lot of background of 964

upregulated genes but after normalization with  $G\alpha q+JQ1$ , the response was more targeted with 38 genes (**Figure 3.6C**).

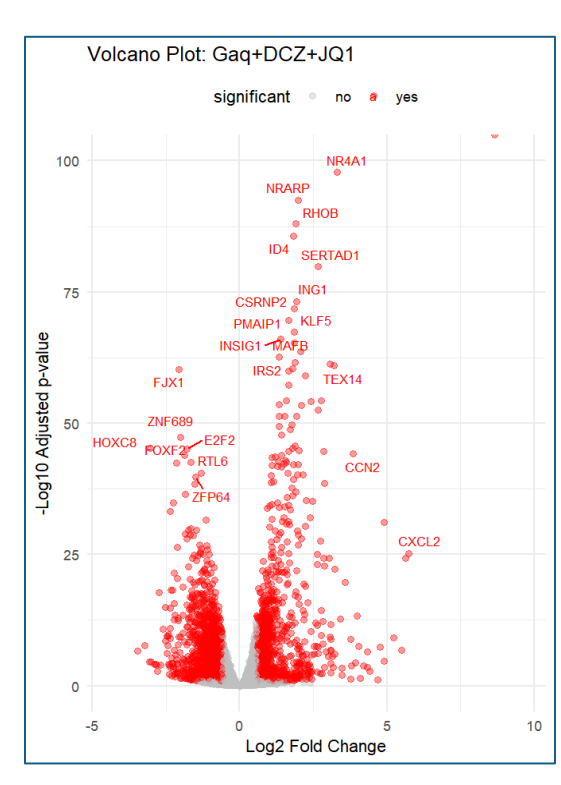
In case of dBET6, without receptor activation ( $G\alpha q + dBET6$ ), the inhibitor itself causes widespread expression changes, with 503 significant genes (**Figure 3.6D**). The receptor activation normalized to DMSO causes a widespread expression of a total of 645 genes. However, when we normalize receptor activation ( $G\alpha q + DCZ + dBET6$ ) to  $G\alpha q + dBET6$ , a lot of background noise was eliminated and a total of 49 genes were expressed (**Figure 3.6F**).

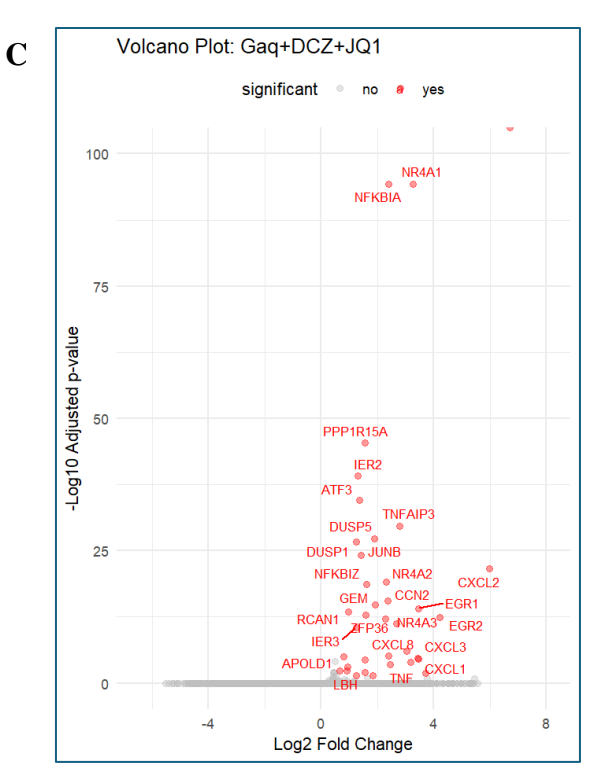
Figure 3.6.



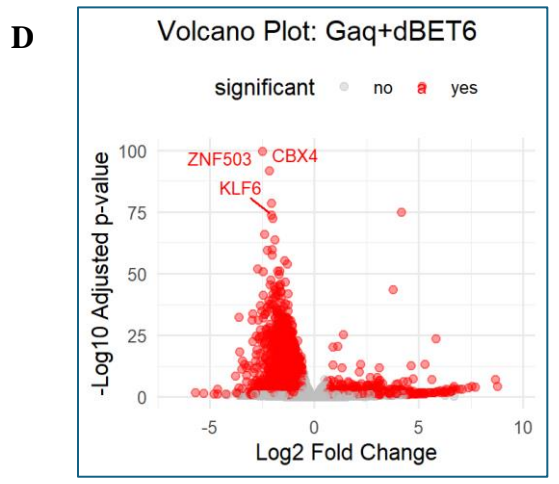


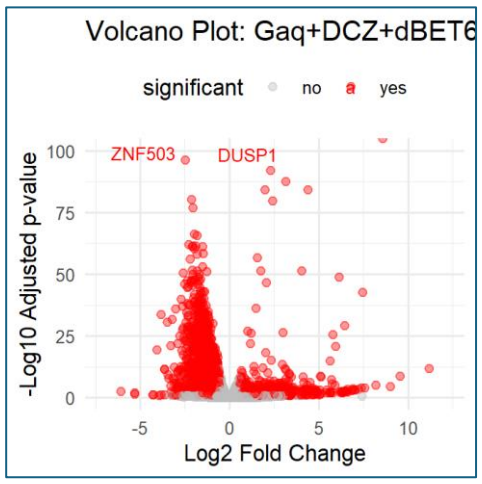
# В

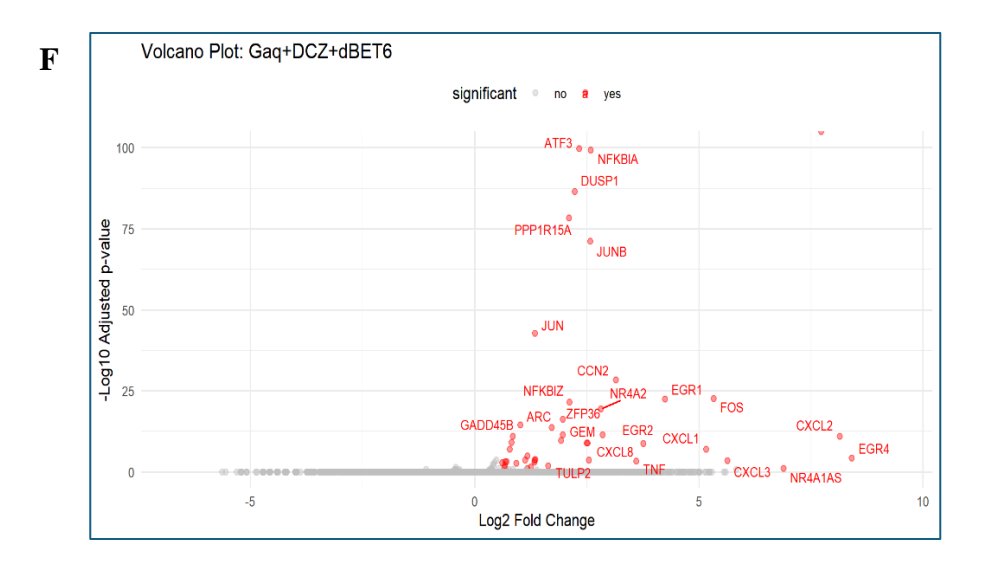




 $\mathbf{E}$ 







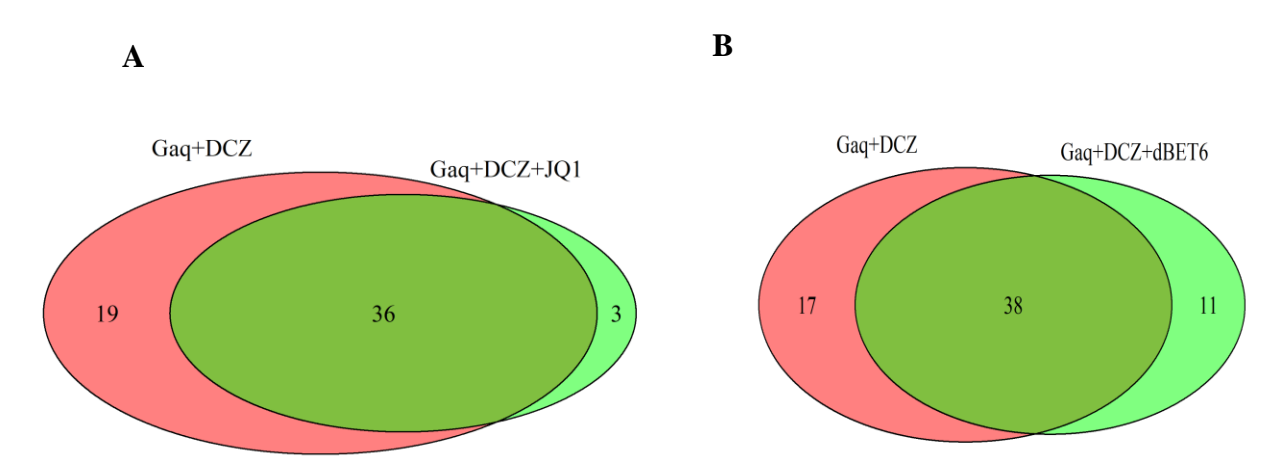
3.6. Volcano plots depict upregulated genes with and without the activation of indicated G protein. (A) depicts the gene expression changes after  $G\alpha q + DCZ$  treatment. The x-axis represents log2fold change, and the y-axis indicates -log10 adjusted p-value. Some of the significantly upregulated genes were: ID4, NR4A2, and SERTAD1. On the other hand, FJX1, INHBB and E2F2 were the ones significantly downregulated. (B) shows gene expression changes after  $G\alpha s + DCZ + JQ1$  treatment. Most of the genes significantly upregulated were somewhat similar to what was observed in the  $G\alpha q + DCZ$  treatment with some exceptions. (C) shows gene expression changes after  $G\alpha s + DCZ + JQ1$  treatment which is normalized to  $G\alpha q + DCZ$  treatment. The key genes upregulated by  $G\alpha s + DCZ + JQ1$  were: NR4A1, NFKB1. (D) depicts the volcano plot of  $G\alpha q + dBET6$  normalized to DMSO. (E) volcano plot shows the gene expression of  $G\alpha q + DCZ + dBET6$  normalized to DMSO. (F) this shows the volcano plot for the genes expressed by  $G\alpha q + DCZ + dBET6$  normalized to  $G\alpha q + dBET6$ . Genes upregulated were significant by p adj. < 0.1 and logfc > 1.

To evaluate the number of genes affected by DCZ in the presence of BET inhibitors, we compared the  $G\alpha q+DCZ+JQ1$  treatment to  $G\alpha q+JQ1$ . A volcano plot was generated for  $G\alpha q+DCZ+JQ1$ , normalized against the  $G\alpha q+JQ1$  treatment, to highlight differential gene expression patterns between these two conditions. In **Figure 3.6C**, we observed, similar number of genes affected as we observed in case of  $G\alpha q+DCZ$  (Figure 3.5A). Similarly, in case of dBET6, the  $G\alpha q+DCZ+dBET6$  treatment (**Figure 3.6E**) was normalized to  $G\alpha q+dBET6$  treatment (**Figure 3.6D**) to produce a more specific gene expression in presence of receptor (**Figure 3.6F**).

## 3.5. Evaluating the effect of BET inhibitors on $G\alpha q$ receptor activation

The upregulated genes shown in  $G\alpha q$  activation and inhibited by JQ1 treatment, were further compared to the  $G\alpha q+DCZ$  condition to assess the inhibitory effect of JQ1 (Figure 3.6A). To better compare the two conditions, Venn diagrams were generated to identify similar and differentially upregulated genes between treatments.

Figure 3.7.



3.7. Venn Diagrams Comparing Two Treatments Highlighting Common and Distinct Gene Expression Patterns. (A) depicts a comparison between two treatments:  $G\alpha q+DCZ$  and  $G\alpha q+DCZ+JQ1$ . The red section represents 19 genes that are inhibited by the JQ1 treatment, while the green section shows three genes specifically upregulated by the  $G\alpha q + DCZ + JQ1$  treatment. (B) Venn diagram compares gene expression between  $G\alpha q + DCZ$  and  $G\alpha q + DCZ + dBET6$  treatments. It shows that 17 genes were inhibited by dBET6, while 11 genes are unique to  $G\alpha q + DCZ + dBET6$  treatment. 38 genes were commonly upregulated in both treatments. Genes upregulated were significant by p adj. < 0.1 and logfc > 0.58.

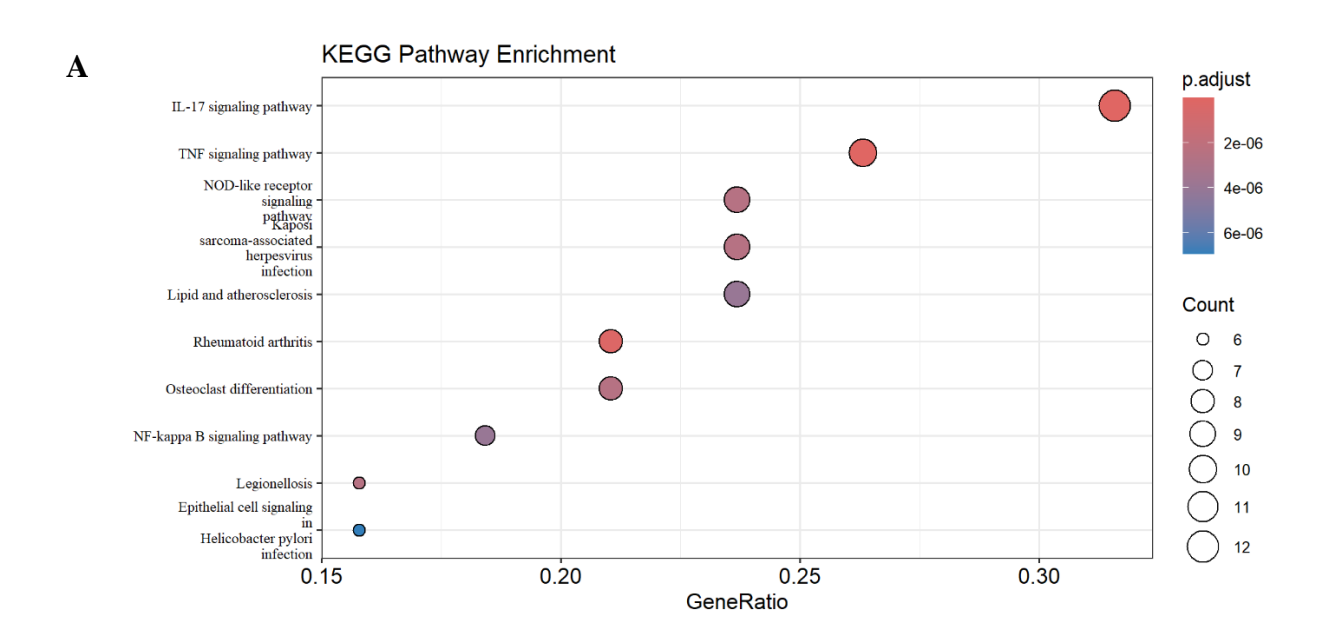
The comparison between the two treatments of  $G\alpha q+DCZ+JQ1$  (normalized to  $G\alpha q+JQ1$ ) in green vs  $G\alpha q+DCZ$  (normalized to  $G\alpha q+DMSO$ ) in red is represented in **Figure 3.7A**. We observed that there were 39 genes that were upregulated in case of  $G\alpha q+DCZ+JQ1$  among which 36 genes were the same as for  $G\alpha q+DCZ$ . Thus, among the 55 upregulated genes in  $G\alpha q+DCZ$ , 36 were upregulated in the presence of inhibitor JQ1 and 19 genes were found to be inhibited by JQ1. Similarly, we also plotted Venn diagram for the treatment of dBET6 upon  $G\alpha q$  activation (**Figure 3.7B**). Here, we can see that there are 49 genes upregulated in the case of  $G\alpha q+DCZ+dBET6$  (normalized to  $G\alpha q+dBET6$ ). It was found that 17 genes were inhibited in the

presence of dBET6 (Figure 3.6B). Together, this suggests that BET inhibitor inhibits a fraction of genes activated by G $\alpha$ q, but that most of genes activated by DCZ in cells expressing the G $\alpha$ q-DREADD were not affected by BET inhibition.

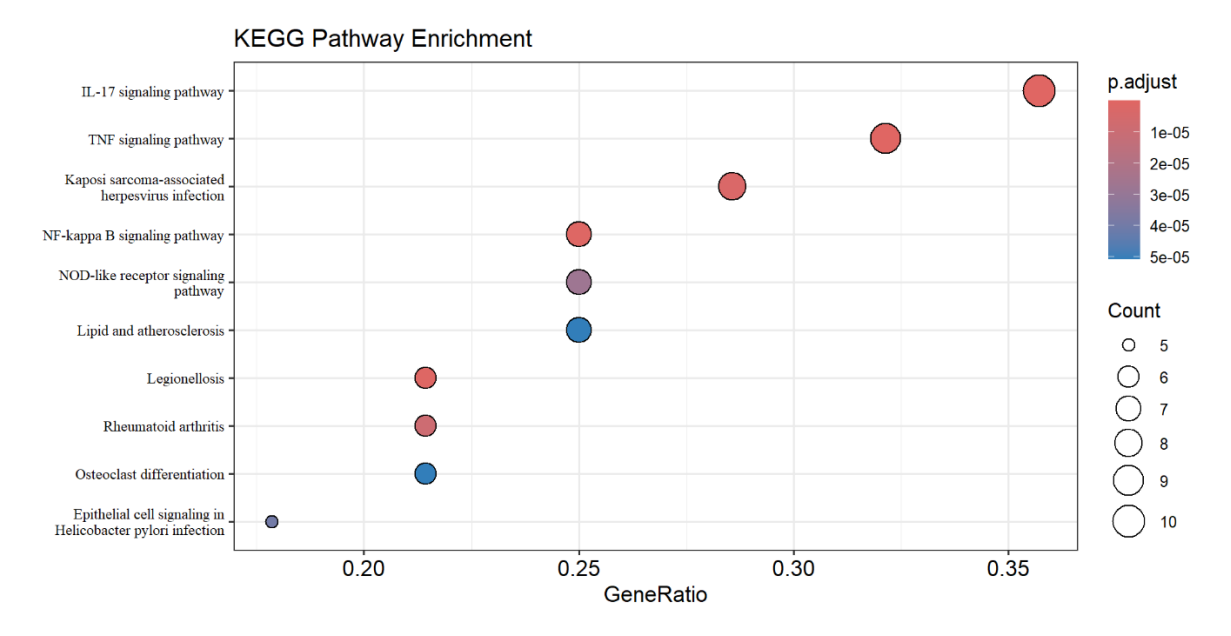
# 3.6. Pathway Enrichment Analysis of genes modulated by BET inhibitors upon Gaq activation.

We conducted an in-depth analysis of the upregulated genes and visualized the gene counts for each KEGG pathway using dot plots to emphasize significant pathways. In these plots, each dot represents a KEGG pathway; the dot size reflects the number of genes associated with the pathway, and the color intensity indicates the significance level (e.g., p-value) of pathway enrichment. **Figure 3.8** illustrates the KEGG pathways associated with the  $G\alpha q+DCZ$  and its effect with BET inhibitor treatment. **Figure 3.8A** shows pathways related to genes upregulated from the  $G\alpha q+DCZ$  condition (Figure 3.5A). **Figure 3.8** (**B & C**) represents the genes inhibited in the presence of JQ1 and dBET6 respectively.

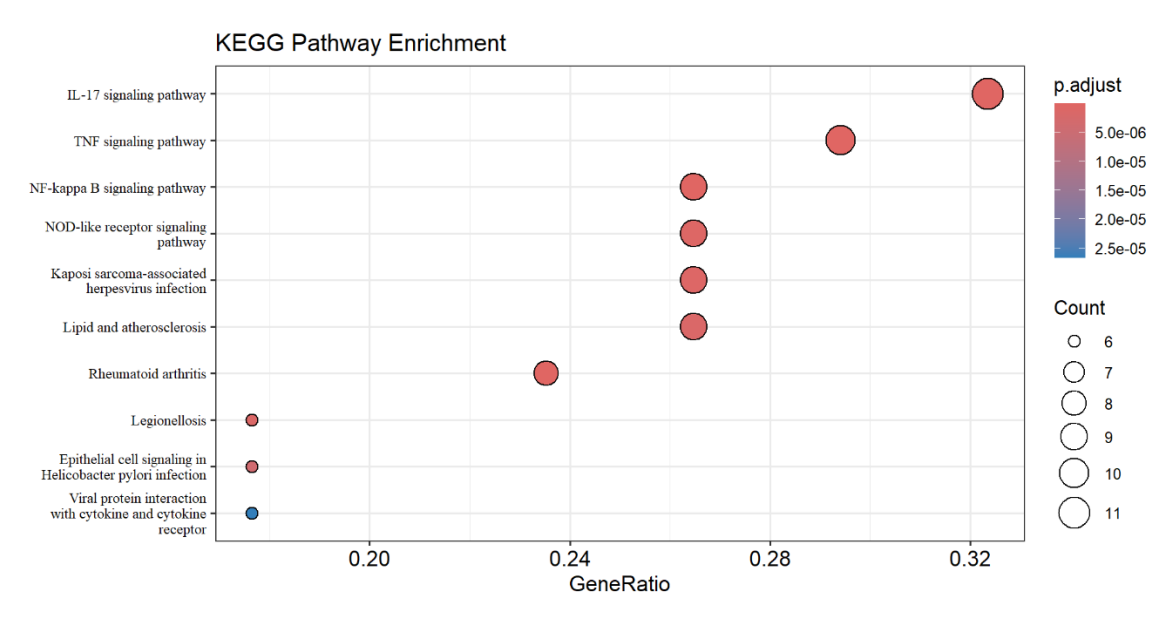
Figure 3.8.



В



C



3.8. KEGG pathway enrichment analysis highlighting key signaling pathways in the presence of inhibitors upon receptor activation. (A) represents the dot plot for the genes upregulated by  $G\alpha q+DCZ$  (Figure 3.6). The x-axis represents the gene ratio, while the y-axis lists enriched pathways. Dot size reflects the number of genes involved (count), and color indicates significance (adjusted p-value), with darker red showing higher significance. (B) represents a dot plot of the  $G\alpha q+DCZ+JQ1$ . The IL-17, NFkB and NOD-like inflammatory pathways seems to have slightly reduced in magnitude. (C) represents a dot plot of  $G\alpha q+DCZ+dBET6$ . Genes upregulated were significant by p adj. < 0.1 and logfc > 0.58.

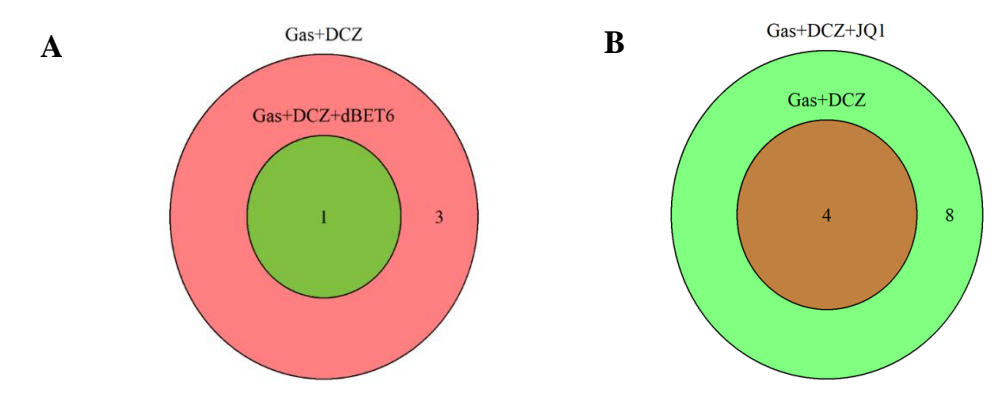
In **Figure 3.8A**, several pathways, including IL-17 signaling, TNF signaling, and NF-kB inflammatory pathways, were significantly enriched. Interestingly, **Figure 3.8B** shows a similar pattern even though it represents the KEGG pathways after the dBET6 treatment. This suggests that the inflammatory pathways were not suppressed in the presence of an inhibitor. JQ1 also seems to show a similar pattern where all the inflammatory pathways were enriched (**Figure 3.8C**). Together, these findings suggest that the activation of genes associated with inflammatory pathways by Gαq signaling is not inhibited by BET inhibitors.

### 3.7. Evaluating the effect of BET inhibitors on Gas activation

In case of G $\alpha$ s activation as observed in the initial volcano plot (**Figure 3.5B**), only four genes were found to be significantly upregulated. We compared G $\alpha$ s+DCZ to G $\alpha$ s+DCZ+dBET6 to know the effect of the inhibitor on the G $\alpha$ s-mediated effects. G $\alpha$ s+DCZ+dBET6 and G $\alpha$ s+DCZ+JQ1 was further normalized to treatments G $\alpha$ s+dBET6 and G $\alpha$ s+JQ1 respectively.

When we compared  $G\alpha s+DCZ+dBET6$  (normalized to  $G\alpha s+dBET6$ ) to  $G\alpha s+DCZ$  (normalized to  $G\alpha s+DMSO$ ), it was found that three of the four genes upregulated by DCZ were not upregulated in the presence dBET6, whereas one of them still was (**Figure 3.9A**). When we compared the treatments for JQ1, i.e.,  $G\alpha s+DCZ+JQ1$  (normalized to  $G\alpha s+JQ1$ ) to  $G\alpha s+DCZ$  (normalized to  $G\alpha s+DMSO$ ) it was found that all of the genes induced by DCZ alone were still induced in the presence of JQ1, and in fact, an additional eight genes were induced as well (**Figure 3.9B**).

Figure 3.9.



C D

ensembl_symbol	log2FoldChange
DUSP1	1.05
PCK1	2.60
NR4A2	1.72
FOS	2.15

ensembl_symbol	log2FoldChange
DUSP1	0.91

 $\mathbf{E}$ 

ensembl_symbol	log2FoldChange (w.r.t Gaq+dBET6)	log2FoldChange (w.r.t DMSO)
NR4A1	3.71	3.14
PCK1	1.17	1.60
FOSB	7.73	8.58
NFKBIZ	2.12	1.34
NR4A2	2.82	1.18
TENT5B	1.13	0.33
RCAN1	0.82	0.65
BTG2	1.34	-0.03
IER2	3.00	1.99
CXCL8	2.50	2.97
FOS	5.33	7.44
JUNB	2.57	2.04

3.9. Analyzing the effect of BET inhibitor on Gas Activation. (A) represents the Venn diagram depicting a comparison between Gas+DCZ and Gas+DCZ+dBET6 treatments where three genes were inhibited by dBET6. (B) represents a comparison between the treatment groups Gas+DCZ and Gas+DCZ+JQ1 where none of the genes were inhibited by JQ1. (C) represents the four genes upregulated by Gas with their logfc. (D) depicts the one gene insensitive to the dBET6 treatment (E) represents some of the genes upregulated by Gaq+DCZ+dBET6 treatment. The yellow highlighted genes are the genes inhibited by dBET6 in case of Gas. Genes upregulated were significant by p adj. < 0.1 and logfc > 0.58.

Since a total of four genes were upregulated upon G $\alpha$ s activation (**Figure 3.9C**), the one gene insensitive to dBET6 treatment was found to be DUSP1 (**Figure 3.9D**). The three genes which were inhibited by dBET6 were PCK1, NR4A2, and FOS. Interestingly, these genes were also among those upregulated by G $\alpha$ q activation but remained unaffected by dBET6 (highlighted in yellow, **Figure 3.9E**).

Our data reveal distinct patterns in gene expression upon DREADD activation with DCZ. Although receptor activation surprisingly regulated only a small number of genes for both G $\alpha$ s and G $\alpha$ q, it provided valuable insights into gene expression in the presence of BET inhibitors. Specifically, genes activated by G $\alpha$ q were largely insensitive to BET inhibitors, particularly dBET6. KEGG pathway analysis of G $\alpha$ q-activated genes suggests that BET inhibitors did not suppress inflammatory pathways, contrary to findings in other studies.

On the other hand, G $\alpha$ s-mediated receptor's gene expression changes were limited, indicating that G $\alpha$ q is likely a more important driver of gene expression in these conditions. However, we identified three genes activated by G $\alpha$ s that were inhibited by BET inhibitors, a pattern not observed for G $\alpha$ q, suggesting that G $\alpha$ s receptor-expressed genes may rely more on Brd4 than those expressed by G $\alpha$ q. These results point to a differential gene expression profile between G $\alpha$ s and G $\alpha$ q receptors, suggesting that further investigation is needed.

#### DISCUSSION

# 4.1 Establishment of a DREADD-based system to monitor gene expression responses to $G\alpha q$ and $G\alpha signaling$

This study investigated how G protein-coupled receptor (GPCR) signaling pathways specifically those mediated by Gas and Gaq proteins differentially affect gene expression, with a focus on Brd4-dependent transcriptional regulation. GPCR pathways are essential for cellular signal transduction, regulating gene expression by initiating diverse signaling cascades that ultimately modulate transcription factors and chromatin modifiers such as Brd4. However, it is still unclear how specific activation of these pathways via Gas or Gaq following GPCR activation differentially influences Brd4-mediated gene transcription, an area that has significant implications for understanding a broader role for Brd4 in gene regulation.

To address this knowledge gap, I used Designer Receptors Exclusively Activated by Designer Drugs (DREADDs), which are engineered receptors that can be activated by synthetic ligands that do not interact with endogenous receptors. This system allows for highly selective and temporally controlled activation of specific G protein-mediated pathways<sup>121,124</sup>. It is thus ideal for studying the distinct effects of Gαs and Gαq activation on Brd4-dependent gene expression. DREADDs have been used extensively to modulate neural circuits and control behaviors<sup>120,122</sup>, but their application to study transcriptional responses has been limited<sup>148</sup>. By applying DREADD technology to transcriptional regulation in combination with BET inhibitors, we can systematically compare the transcriptional outcomes of activating Gαs versus Gαq pathways in a Brd4-dependent context.

### 4.1.1 Observations and challenges

We initially used the synthetic ligand DCZ due to its high selectivity and potency for the DREADDs we used<sup>4,5</sup>. However, when analyzing gene expression through RNA sequencing, we observed that relatively few genes were activated following DREADD stimulation. We had anticipated that many more genes would be affected by  $G\alpha q$  or  $G\alpha s$  activation, although the reasons for the gene selectivity are currently unclear. It is possible that this could be due to the length of time for DCZ treatment. GPCR signaling often induces rapid but transient effects in pathways mediated by  $G\alpha s$  and  $G\alpha q$ . For instance, in our bioluminescence resonance energy transfer (BRET) experiments, we saw that  $G\alpha s$  signaling reached its peak activation within

approximately 10 minutes, after which the signal diminished by the 1-hour mark. This decrease in effectiveness suggests that longer times might have been necessary beyond the 1h stimulation followed by RNA sequencing. We might have missed the peak transcriptional response.

The limited gene activation could be due to several factors. GPCRs are known to undergo desensitization, internalization, and feedback inhibition over time<sup>153</sup>, which can decrease the receptor's signaling activity and thereby dampen downstream gene activation. Desensitization occurs when prolonged receptor activation leads to phosphorylation of the receptor, reducing its ability to productively couple with G proteins<sup>154</sup>, while internalization removes the receptor from the cell surface<sup>155</sup>, further reducing its activity.

### 4.1.2 Optimizing the DREADD system

To address this, we could conduct additional experiments using different DCZ treatment times to better capture the early, peak, and late-transcriptional responses. Shorter treatment windows (e.g., 5–30 minutes) would allow us to isolate the initial gene expression events that occur at different times of Gαs or Gαq activation, potentially revealing a broader spectrum of genes influenced by Brd4 in response to each pathway.

By performing RNA sequencing at multiple time points, we should be able capture distinct phases of transcriptional activity and gain a more comprehensive understanding of the early and later transcriptional networks regulated by Gas and Gaq signaling through Brd4. This approach could uncover pathway-specific gene regulatory networks and provide new insights into how distinct GPCR pathways engage Brd4 to drive different transcriptional outcomes.

In summary, this study applies DREADD technology to dissect the transcriptional consequences of Gas and Gaq signaling on Brd4-mediated gene expression, an approach that could reveal pathway-specific gene networks. Optimizing treatment timing and exploring pathway-specific roles of Brd4 which will help shed light on the nuances of GPCR-regulated transcription, potentially aid in the development of targeted therapies for diseases associated with Brd4 and GPCR signaling.

This study provides valuable insights into the differential gene expression profiles resulting from Gαs and Gαq receptor activation, highlighting the complex interplay between BET inhibition, transcriptional regulation, and pathway-specific engagement with transcriptional complexes such as Brd4 and the super elongation complex (SEC).

### 4.2 Differential gene expression upon $G\alpha$ s and $G\alpha$ g receptors activation.

Our findings indicate that  $G\alpha q$  signaling led to the activation of 55 genes, while  $G\alpha s$  signaling activated only four. This difference in gene activation suggests that these pathways engage in different transcriptional mechanisms or regulatory networks. Whereas DREADD activation was associated with differential expression of relatively small numbers of genes in our system, treatment with we observed that BET inhibitors such as dBET6 and JQ1, introduced substantial background noise in gene expression by inducing a broad spectrum of genes unrelated to receptor activation. This unintended effect presented a challenge for isolating receptor-specific gene activation, prompting us to normalize our data to exclude genes solely induced by BET inhibitors and instead focus on those specifically activated by the receptors and simultaneously suppressed by BET inhibitors. However, this normalization was challenging for  $G\alpha s$ , given the limited number of genes activated, which limited statistical power.

### 4.2.1 BET inhibition and Brd4 dependency in Gaq- and Gas-mediated gene activation

Using Venn diagrams, we quantified BET-inhibited genes activated by both G proteins, revealing patterns that suggest pathway-specific dependencies on Brd4. For G $\alpha$ q+DCZ treatment (normalized to DMSO) compared to G $\alpha$ q+DCZ+dBET6/JQ1 (normalized to G $\alpha$ q+dBET6/JQ1), we observed consistent gene upregulation across treatments, indicating that G $\alpha$ q-induced gene activation is largely Brd4-independent. This suggests that G $\alpha$ q signaling may predominantly involve the SEC component of P-TEFb rather than the P-TEFb-Brd4 complex. This finding is similar to our previous work on differential activation of P-TEFb complexes in cardiac hypertrophy<sup>119</sup>.

Additionally, a small number of genes activated by Gas showed sensitivity to BET inhibition by dBET6, indicating a reliance on Brd4. Interestingly, these Gas-induced genes were unresponsive to dBET6 when activated through Gaq, highlighting a key distinction in the dependence on Brd4 between the two signaling pathways.

### 4.2.2 Distinct mechanisms of dBET6 and JQ1 in gene regulation

Our data further suggests distinct mechanisms of action between dBET6 and JQ1. Notably, JQ1 did not inhibit Gas-activated genes as dBET6 did. Instead, JQ1 appeared to activate additional genes, the reason for which is still not clear. This differential activity may indicate that dBET6 and

JQ1 interact with BRD4 or associated complexes in unique ways, where dBET6 inhibits Brd4 more specifically in a way that impacts Gαs-upregulated genes. Conversely, JQ1 may exert broader effects on transcriptional regulation, possibly by engaging transcription elongation factors that bypass Brd4's role, thus activating alternative gene sets. This observation underlines the complexity of BET inhibitors and their pathway-specific interactions.

### 4.2.3 Comparison to prior lab findings in cardiac hypertrophy models

These findings support our previous research, which demonstrated that G $\alpha$ q-driven transcription in cardiac hypertrophy is more dependent on the P-TEFb-SEC complex, while G $\alpha$ s-driven transcription requires the P-TEFb-Brd4 complex<sup>119</sup>. In our cardiac hypertrophy models, hypertrophic stimulation via  $\alpha_1$ -adrenergic receptors ( $\alpha_1$ -AR) activated both G $\alpha$ s and G $\alpha$ q signaling whereas endothelin receptor (ETR) activated G $\alpha$ q signaling<sup>119</sup>. SEC knockdown attenuated hypertrophy driven by both  $\alpha_1$ -AR and ETR agonists, while BET inhibition using JQ1 reduced hypertrophy only in  $\alpha_1$ -AR-stimulated cells, not in those stimulated by ETR agonists. These data highlight that G $\alpha$ s-driven hypertrophy is Brd4-dependent, whereas G $\alpha$ q-driven hypertrophy bypasses Brd4, instead utilizing SEC<sup>119</sup>.

Further, protein kinase A (PKA) inhibition reduced the expression of hypertrophic marker genes, suggesting that Gαs activates Brd4 through a cAMP/PKA-dependent mechanism<sup>119</sup>. This finding implies that PKA may phosphorylate Brd4 directly or indirectly through its cofactors, contributing to Brd4 activation and gene transcription in a pathway-specific manner. Our future research aims to clarify these mechanisms by performing Brd4 chromatin immunoprecipitation (ChIP) in response to DREADD activation in HEK 293 cells. If Brd4 chromatin occupancy is found to be PKA-sensitive in this system, it would imply that Gαs and PKA signaling may be generally important for Brd4 to act at its transcriptional targets. Such a finding could be tested in other physiological contexts in which Brd4 function has been characterized. It could have important implications for the development of BET inhibitors as therapies.

### 4.3. Effects of BET Inhibitors on Inflammatory Pathways

In our study, we investigated the impact of two different BET inhibitors, JQ1 and dBET6, on inflammatory pathway regulation and transcriptional mechanisms in HEK cells<sup>156</sup>. BET proteins, especially Brd4, are key players in transcriptional regulation due to their interactions with

acetylated lysines on chromatin, which enables them to recruit transcriptional machinery to gene regulatory regions, including those associated with inflammation<sup>156</sup>. Both JQ1 and dBET6 target BET proteins, but through different mechanisms, leading to distinct effects on gene expression and inflammatory signaling.

### 4.3.1 Mechanisms of JQ1 and dBET6 in transcriptional regulation

JQ1 is a well-characterized bromodomain inhibitor that competes with acetylated lysines, blocking BET proteins from binding to chromatin<sup>157</sup>. This inhibition is particularly impactful at super-enhancers—large regulatory regions enriched with transcriptional machinery that control the expression of genes essential for maintaining cell identity and those involved in disease processes, such as inflammatory cytokines<sup>156</sup>. By inhibiting bromodomain-mediated interactions, JQ1 disrupts mediator-Brd4 complexes that play a crucial role at super-enhancer sites, which in turn affects transcriptional elongation factors like P-TEFb<sup>111,158</sup>. As a result, JQ1 broadly suppresses transcription driven by super-enhancers, leading to an attenuation of gene expression related to inflammation and other disease pathways.

In contrast, dBET6 operates through a different mechanism known as targeted protein degradation. Rather than simply blocking bromodomains, dBET6 causes the ubiquitination and proteasomal degradation of Brd4<sup>144</sup>. This approach eliminates Brd4 from chromatin, preventing its recruitment of essential transcriptional regulators like SPT5, NELF, and MED1<sup>144</sup>. By removing Brd4, dBET6 disrupts the chromatin-associated complexes more comprehensively, leading to reduced phosphorylation of RNA polymerase II at Ser2, a modification critical for transcriptional elongation<sup>144</sup>. This mechanism implies that dBET6 could have broader effects on transcription compared to JQ1, as it not only inhibits Brd4 binding but also dismantles Brd4-dependent chromatin complexes.

### 4.3.2 Divergent effects of JQ1 and dBET6 on inflammatory pathways and c-myc Activation

BET inhibitors have been widely researched for their potential to suppress inflammation in diseases characterized by excessive cytokine production, such as rheumatoid arthritis, cancer, and cardiovascular disease. BET inhibition, especially through compounds like JQ1, is often thought to dampen inflammatory gene expression by preventing transcriptional activation at

inflammation-associated super-enhancers<sup>4</sup>. However, our findings challenge this assumption. In our HEK cell model, we observed that JQ1 did not significantly suppress inflammatory pathways as anticipated. Instead, JQ1 treatment led to an increase in c-Myc expression, which may contribute to the observed rise in inflammatory activity.

Elevated c-Myc levels have been shown to activate pro-inflammatory genes, contributing to the expression of cytokines like IL-1, TNF, and pathways involving NF-κB<sup>146-149</sup>. This upregulation could mean that, rather than uniformly suppressing inflammation, JQ1 can, under certain conditions, actually promote inflammatory gene expression by enhancing c-Myc activity. The effect of c-Myc activation observed with JQ1 but not with dBET6 (**Figure S3**) suggests that mechanism of bromodomain inhibition by JQ1 may drive inflammation via a P-TEFb-independent manner, possibly due to its selective disruption of BET protein-chromatin interactions rather than the broader impact of Brd4 degradation seen with dBET6.

### 4.3.3 Implications for BET Protein Function in Inflammatory Pathway Regulation

Our findings suggest that BET inhibition does not yield uniform anti-inflammatory effects across all contexts. The differences between JQ1 and dBET6 indicate that BET proteins might regulate inflammatory pathways through both P-TEFb-dependent and independent mechanisms. Bromodomain inhibition by JQ1 affects P-TEFb recruitment and transcriptional elongation differently in comparison to dBET6, which degrades Brd4 and more comprehensively removes its transcriptional functions. While dBET6-induced degradation of Brd4 disrupts transcriptional factors (like c-myc) more effectively, the bromodomain-inhibition by JQ1 may cause the stimulation of certain transcription factors like c-Myc. However, in our results, both lead to an increase in inflammatory pathways.

The inflammatory effects seen in HEK cells with BET inhibition may differ from those in disease-relevant contexts. It is possible that BET inhibition elevates pro-inflammatory genes under specific conditions in HEK cells while exerting an anti-inflammatory effect in disease states. For instance, the role of Brd4 in inflammation may vary depending on cellular environment, stress signals, or disease stage, highlighting a case-specific regulatory function for BET proteins. This could imply that, while BET inhibition has anti-inflammatory potential in certain settings, it might activate pro-inflammatory pathways in others, depending on the broader signaling context.

### 4.4. Conclusion and Implications of Brd4

In summary, our data suggests a differential activation of G proteins involved in Brd4 activation. We validated our previous findings on the Gαs-dependent activation of Brd4. Additionally, we concluded that genes stimulated by Gαq remain unaffected by BET inhibitors, suggesting that the downstream effects of Gαq signaling are largely independent of Brd4. Furthermore, we observed that these inhibitors did not suppress inflammatory processes. Interestingly, JQ1 treatment was associated with increased c-Myc levels; however, the underlying mechanism remains unclear. Further studies in cardiomyocyte models will be essential to understanding the regulation of G protein signaling pathways and inflammatory pathways in cardiac hypertrophy. By elucidating these mechanisms, we aim to uncover new therapeutic strategies targeting Brd4 to modulate inflammation and transcriptional responses in cardiovascular disease.

### **FUTURE DIRECTIONS**

To further elucidate receptor-specific transcriptional mechanisms, we propose several experimental strategies. In HEK 293 cells, chromatin immunoprecipitation followed by quantitative PCR (ChIP-qPCR) will be employed to analyze Brd4's occupancy at selected target genes identified from RNA sequencing data, such as PCK1, NR4A2, and FOS. These experiments could provide insight into Brd4 recruitment to target genes specifically activated by Gαs or Gαq signaling. To refine our approach, we can incorporate SEC inhibitors alongside ChIP-qPCR, enabling us to dissect the contributions of Brd4 and the super elongation complex (SEC) to transcriptional regulation mediated by Gαs and Gαq. This could illuminate how distinct GPCR pathways modulate P-TEFb complexes and their associated transcriptional networks.

In the context of cardiovascular diseases, these inflammatory responses are particularly relevant to conditions such as heart failure, where cytokine production and inflammatory signaling increase during cardiac remodeling and hypertrophy. Chronic inflammation contributes to pathological remodeling in heart failure, underscoring the importance of understanding how Brd4 and BET inhibitors affect inflammatory pathways in cardiac contexts. Expanding our studies to cardiomyocytes could provide deeper insights into Brd4's role in cardiomyocyte inflammation and hypertrophy. We propose the use of rat neonatal cardiomyocytes or human induced pluripotent stem cell (iPSC)-derived cardiomyocytes as disease models. These cell types could allow us to examine how Brd4 and SEC contribute to GPCR-mediated inflammatory and hypertrophic responses, which are central to cardiac pathology.

Additionally, investigating the influence of BET inhibitors such as JQ1 and dBET6 on GPCR pathways in cardiomyocytes could clarify how Brd4-dependent transcription is regulated during cardiac hypertrophy. GPCR signaling pathways are critical for cardiomyocyte function and are implicated in hypertrophic gene expression. These studies can include ChIP-qPCR experiments to measure the recruitment of Brd4 to specific inflammatory and hypertrophic target genes, aiding in our understanding of how Brd4 coordinates tissue-specific inflammatory and hypertrophic responses. BET inhibitors' potential to modulate these responses in heart disease will also be assessed.

To enhance the precision of our studies, we can integrate nascent transcript analysis methods in combination with Designer Receptors Exclusively Activated by Designer Drugs (DREADDs).

This approach would allow us to directly assess transcriptional responses and transcription factor recruitment with greater accuracy than traditional RNA-seq or ChIP-seq techniques. By leveraging DREADDs, we could observe pathway-specific activation and its immediate effects on transcription, providing a dynamic view of GPCR-mediated transcriptional regulation.

In the long term, our research aims to delineate the distinct roles of Brd4 and SEC in  $G\alpha s$  and  $G\alpha q$  signaling. These efforts could uncover novel regulatory mechanisms and identify potential therapeutic targets within these pathways. Such insights may significantly impact the development of strategies targeting cardiovascular diseases and other conditions where GPCR signaling and Brd4 play critical roles.

### REFERENCES

- 1. Heart Wikipedia. Accessed December 3, 2024. https://en.wikipedia.org/wiki/Heart
- 2. Heart disease Symptoms and causes. Mayo Clinic. Accessed December 11, 2024. https://www.mayoclinic.org/diseases-conditions/heart-disease/symptoms-causes/syc-20353118
- 3. Disease C and MP of C. The Pathophysiology of Cardiac Hypertrophy and Heart Failure. Clinical Tree. September 17, 2023. Accessed September 13, 2024. https://clinicalpub.com/the-pathophysiology-of-cardiac-hypertrophy-and-heart-failure/
- 4. Government of Canada SC. The Daily Deaths, 2021. August 28, 2023. Accessed October 4, 2023. https://www150.statcan.gc.ca/n1/daily-quotidien/230828/dq230828beng.htm
- 5. Canada PHA of. Heart Disease in Canada. February 10, 2017. Accessed August 19, 2024. https://www.canada.ca/en/public-health/services/publications/diseases-conditions/heart-disease-canada.html
- 6. Canadian Chronic Disease Surveillance System (CCDSS). Accessed August 19, 2024. https://health-infobase.canada.ca/ccdss/data-tool/Index?G=00&V=9&M=5&Y=2017
- 7. Cardiovascular diseases (CVDs). Accessed August 20, 2024. https://www.who.int/news-room/fact-sheets/detail/cardiovascular-diseases-(cvds)
- 8. Benjamin EJ, Blaha MJ, Chiuve SE, et al. Heart Disease and Stroke Statistics—2017 Update. *Circulation*. 2017;135(10):e146-e603. doi:10.1161/CIR.0000000000000485
- 9. Dario Diviani group. Accessed September 7, 2024. https://www.unil.ch/dsb/en/home/menuinst/groupes-de-recherche/dario-diviani.html
- 10. Cohn JN, Ferrari R, Sharpe N. Cardiac remodeling—concepts and clinical implications: a consensus paper from an international forum on cardiac remodeling. *Journal of the American College of Cardiology*. 2000;35(3):569-582. doi:10.1016/S0735-1097(99)00630-0
- 11. Arai M, Yoguchi A, Iso T, et al. Endothelin-1 and its binding sites are upregulated in pressure overload cardiac hypertrophy. *American Journal of Physiology-Heart and Circulatory Physiology*. 1995;268(5):H2084-H2091. doi:10.1152/ajpheart.1995.268.5.H2084
- 12. Schunkert H, Dzau VJ, Tang SS, Hirsch AT, Apstein CS, Lorell BH. Increased rat cardiac angiotensin converting enzyme activity and mRNA expression in pressure overload left ventricular hypertrophy. Effects on coronary resistance, contractility, and relaxation. *J Clin Invest*. 1990;86(6):1913-1920. doi:10.1172/JCI114924

- 13. Yamazaki T, Komuro I, Yazaki Y. Role of the renin-angiotensin system in cardiac hypertrophy. *The American Journal of Cardiology*. 1999;83(12, Supplement 1):53-57. doi:10.1016/S0002-9149(99)00259-3
- 14. Yayama K, Horii M, Hiyoshi H, et al. Up-Regulation of Angiotensin II Type 2 Receptor in Rat Thoracic Aorta by Pressure-Overload. *J Pharmacol Exp Ther*. 2004;308(2):736-743. doi:10.1124/jpet.103.058420
- 15. Pierce KL, Premont RT, Lefkowitz RJ. Seven-transmembrane receptors. *Nat Rev Mol Cell Biol*. 2002;3(9):639-650. doi:10.1038/nrm908
- 16. Neves SR, Ram PT, Iyengar R. G protein pathways. *Science*. 2002;296(5573):1636-1639. doi:10.1126/science.1071550
- 17. Wang J, Gareri C, Rockman HA. G-Protein-Coupled Receptors in Heart Disease. *Circ Res.* 2018;123(6):716-735. doi:10.1161/CIRCRESAHA.118.311403
- 18. Rockman HA, Koch WJ, Lefkowitz RJ. Seven-transmembrane-spanning receptors and heart function. *Nature*. 2002;415(6868):206-212. doi:10.1038/415206a
- Hill JA, Olson EN. Cardiac plasticity. N Engl J Med. 2008;358(13):1370-1380. doi:10.1056/NEJMra072139
- 20. Tham YK, Bernardo BC, Ooi JYY, Weeks KL, McMullen JR. Pathophysiology of cardiac hypertrophy and heart failure: signaling pathways and novel therapeutic targets. *Arch Toxicol*. 2015;89(9):1401-1438. doi:10.1007/s00204-015-1477-x
- 21. Rapacciuolo A, Esposito G, Caron K, Mao L, Thomas SA, Rockman HA. Important role of endogenous norepinephrine and epinephrine in the development of in vivo pressure-overload cardiac hypertrophy. *Journal of the American College of Cardiology*. 2001;38(3):876-882. doi:10.1016/S0735-1097(01)01433-4
- 22. Kankanamge D, Ubeysinghe S, Tennakoon M, et al. Dissociation of the G protein βγ from the Gq–PLCβ complex partially attenuates PIP2 hydrolysis. *Journal of Biological Chemistry*. 2021;296:100702. doi:10.1016/j.jbc.2021.100702
- 23. Bernardo BC, Weeks KL, Pretorius L, McMullen JR. Molecular distinction between physiological and pathological cardiac hypertrophy: Experimental findings and therapeutic strategies. *Pharmacology & Therapeutics*. 2010;128(1):191-227. doi:10.1016/j.pharmthera.2010.04.005
- 24. Hubbard KB, Hepler JR. Cell signalling diversity of the Gqα family of heterotrimeric G proteins. *Cellular Signalling*. 2006;18(2):135-150. doi:10.1016/j.cellsig.2005.08.004
- 25. D'Angelo DD, Sakata Y, Lorenz JN, et al. Transgenic Galphaq overexpression induces cardiac contractile failure in mice. *Proc Natl Acad Sci U S A*. 1997;94(15):8121-8126. doi:10.1073/pnas.94.15.8121

- 26. Mende U, Kagen A, Cohen A, Aramburu J, Schoen FJ, Neer EJ. Transient cardiac expression of constitutively active Galphaq leads to hypertrophy and dilated cardiomyopathy by calcineurin-dependent and independent pathways. *Proc Natl Acad Sci U S A*. 1998;95(23):13893-13898. doi:10.1073/pnas.95.23.13893
- 27. Salazar NC, Chen J, Rockman HA. Cardiac GPCRs: GPCR signaling in healthy and failing hearts. *Biochimica et Biophysica Acta (BBA) Biomembranes*. 2007;1768(4):1006-1018. doi:10.1016/j.bbamem.2007.02.010
- 28. McKinsey TA, Olson EN. Toward transcriptional therapies for the failing heart: chemical screens to modulate genes. *J Clin Invest*. 2005;115(3):538-546. doi:10.1172/JCI24144
- 29. Cameron VA, Ellmers LJ. Minireview: Natriuretic Peptides during Development of the Fetal Heart and Circulation. *Endocrinology*. 2003;144(6):2191-2194. doi:10.1210/en.2003-0127
- 30. Katz AM. *Physiology of the Heart*. Wolters Kluwer Health/Lippincott Williams & Wilkins Health; 2011. https://books.google.co.in/books?id=9Am0vQEACAAJ
- 31. Gorski PA, Ceholski DK, Hajjar RJ. Altered myocardial calcium cycling and energetics in heart failure--a rational approach for disease treatment. *Cell Metab*. 2015;21(2):183-194. doi:10.1016/j.cmet.2015.01.005
- 32. Periasamy M, Bhupathy P, Babu GJ. Regulation of sarcoplasmic reticulum Ca2+ ATPase pump expression and its relevance to cardiac muscle physiology and pathology. *Cardiovascular Research*. 2007;77(2):265-273. doi:10.1093/cvr/cvm056
- 33. Kawase Y, Ly HQ, Prunier F, et al. Reversal of cardiac dysfunction after long-term expression of SERCA2a by gene transfer in a pre-clinical model of heart failure. *J Am Coll Cardiol*. 2008;51(11):1112-1119. doi:10.1016/j.jacc.2007.12.014
- 34. Kiss E, Ball NA, Kranias EG, Walsh RA. Differential Changes in Cardiac Phospholamban and Sarcoplasmic Reticular Ca <sup>2+</sup> -ATPase Protein Levels: Effects on Ca <sup>2+</sup> Transport and Mechanics in Compensated Pressure-Overload Hypertrophy and Congestive Heart Failure. *Circulation Research*. 1995;77(4):759-764. doi:10.1161/01.RES.77.4.759
- 35. Mørk HK, Sjaastad I, Sande JB, Periasamy M, Sejersted OM, Louch WE. Increased cardiomyocyte function and Ca2+ transients in mice during early congestive heart failure. *Journal of Molecular and Cellular Cardiology*. 2007;43(2):177-186. doi:10.1016/j.yjmcc.2007.05.004
- 36. De Jongh KS, Murphy BJ, Colvin AA, Hell JW, Takahashi M, Catterall WA. Specific phosphorylation of a site in the full-length form of the alpha 1 subunit of the cardiac L-type calcium channel by adenosine 3',5'-cyclic monophosphate-dependent protein kinase. *Biochemistry*. 1996;35(32):10392-10402. doi:10.1021/bi953023c
- 37. Sculptoreanu A, Rotman E, Takahashi M, Scheuer T, Catterall WA. Voltage-dependent potentiation of the activity of cardiac L-type calcium channel alpha 1 subunits due to

- phosphorylation by cAMP-dependent protein kinase. *Proc Natl Acad Sci U S A*. 1993;90(21):10135-10139.
- 38. Antos CL, Frey N, Marx SO, et al. Dilated Cardiomyopathy and Sudden Death Resulting From Constitutive Activation of Protein Kinase A. *Circulation Research*. 2001;89(11):997-1004. doi:10.1161/hh2301.100003
- 39. Herron TJ, McDonald KS. Small Amounts of α-Myosin Heavy Chain Isoform Expression Significantly Increase Power Output of Rat Cardiac Myocyte Fragments. *Circulation Research*. 2002;90(11):1150-1152. doi:10.1161/01.RES.0000022879.57270.11
- 40. Lowes BD, Minobe W, Abraham WT, et al. Changes in gene expression in the intact human heart. Downregulation of alpha-myosin heavy chain in hypertrophied, failing ventricular myocardium. *J Clin Invest*. 1997;100(9):2315-2324. doi:10.1172/JCI119770
- 41. Nakao K, Minobe W, Roden R, Bristow MR, Leinwand LA. Myosin heavy chain gene expression in human heart failure. *J Clin Invest*. 1997;100(9):2362-2370. doi:10.1172/JCI119776
- 42. Lompré AM, Nadal-Ginard B, Mahdavi V. Expression of the cardiac ventricular alpha- and beta-myosin heavy chain genes is developmentally and hormonally regulated. *J Biol Chem*. 1984;259(10):6437-6446.
- 43. Swynghedauw B. Developmental and functional adaptation of contractile proteins in cardiac and skeletal muscles. *Physiological Reviews*. 1986;66(3):710-771. doi:10.1152/physrev.1986.66.3.710
- 44. Machackova J, Barta J, Dhalla NS. Myofibrillar remodelling in cardiac hypertrophy, heart failure and cardiomyopathies. *Canadian Journal of Cardiology*. 2006;22(11):953-968. doi:10.1016/S0828-282X(06)70315-4
- 45. Pope B, Hoh JFY, Weeds A. The ATPase activities of rat cardiac myosin isoenzymes. *FEBS Letters*. 1980;118(2):205-208. doi:10.1016/0014-5793(80)80219-5
- 46. Kemperman H, Van Den Berg M, Kirkels H, De Jonge N. B-Type Natriuretic Peptide (BNP) and N-Terminal proBNP in Patients with End-Stage Heart Failure Supported by a Left Ventricular Assist Device. *Clinical Chemistry*. 2004;50(9):1670-1672. doi:10.1373/clinchem.2003.030510
- 47. Patel JB, Valencik ML, Pritchett AM, Burnett JC, McDonald JA, Redfield MM. Cardiac-specific attenuation of natriuretic peptide A receptor activity accentuates adverse cardiac remodeling and mortality in response to pressure overload. *Am J Physiol Heart Circ Physiol*. 2005;289(2):H777-784. doi:10.1152/ajpheart.00117.2005
- 48. Tamura N, Ogawa Y, Yasoda A, Itoh H, Saito Y, Nakao K. Two cardiac natriuretic peptide genes (atrial natriuretic peptide and brain natriuretic peptide) are organized in tandem in the mouse and human genomes. *J Mol Cell Cardiol*. 1996;28(8):1811-1815. doi:10.1006/jmcc.1996.0170

- 49. Sanchez R, Meslamani J, Zhou MM. The bromodomain: From epigenome reader to druggable target. *Biochimica et Biophysica Acta (BBA) Gene Regulatory Mechanisms*. 2014;1839(8):676-685. doi:10.1016/j.bbagrm.2014.03.011
- 50. Filippakopoulos P, Knapp S. The bromodomain interaction module. *FEBS Letters*. 2012;586(17):2692-2704. doi:10.1016/j.febslet.2012.04.045
- 51. Gillette TG, Hill JA. Readers, Writers, and Erasers: Chromatin as the Whiteboard of Heart Disease. *Circulation Research*. 2015;116(7):1245-1253. doi:10.1161/CIRCRESAHA.116.303630
- 52. Biswas S, Rao CM. Epigenetic tools (The Writers, The Readers and The Erasers) and their implications in cancer therapy. *European Journal of Pharmacology*. 2018;837:8-24. doi:10.1016/j.ejphar.2018.08.021
- 53. Park SY, Kim JS. A short guide to histone deacetylases including recent progress on class II enzymes. *Exp Mol Med*. 2020;52(2):204-212. doi:10.1038/s12276-020-0382-4
- 54. Histone deacetylase signaling in cardioprotection | Cellular and Molecular Life Sciences. Accessed December 11, 2024. https://link.springer.com/article/10.1007/s00018-013-1516-9
- 55. Histone deacetylase (HDAC) inhibitors attenuate cardiac hypertrophy by suppressing autophagy | PNAS. Accessed December 11, 2024. https://www.pnas.org/doi/full/10.1073/pnas.1015081108
- 56. Themes UFO. Left Ventricular Hypertrophy and Failure. Thoracic Key. August 19, 2016. Accessed September 13, 2024. https://thoracickey.com/left-ventricular-hypertrophy-and-failure/
- 57. van Berlo JH, Elrod JW, Aronow BJ, Pu WT, Molkentin JD. Serine 105 phosphorylation of transcription factor GATA4 is necessary for stress-induced cardiac hypertrophy in vivo. *Proc Natl Acad Sci U S A*. 2011;108(30):12331-12336. doi:10.1073/pnas.1104499108
- 58. McKinsey TA, Zhang CL, Olson EN. Activation of the myocyte enhancer factor-2 transcription factor by calcium/calmodulin-dependent protein kinase-stimulated binding of 14-3-3 to histone deacetylase 5. *Proceedings of the National Academy of Sciences*. 2000;97(26):14400-14405. doi:10.1073/pnas.260501497
- 59. McKinsey TA, Zhang CL, Olson EN. MEF2: a calcium-dependent regulator of cell division, differentiation and death. *Trends Biochem Sci.* 2002;27(1):40-47. doi:10.1016/s0968-0004(01)02031-x
- 60. Zhang CL, McKinsey TA, Chang S, Antos CL, Hill JA, Olson EN. Class II Histone Deacetylases Act as Signal-Responsive Repressors of Cardiac Hypertrophy. *Cell*. 2002;110(4):479-488. doi:10.1016/S0092-8674(02)00861-9

- 61. Yanazume T, Hasegawa K, Morimoto T, et al. Cardiac p300 Is Involved in Myocyte Growth with Decompensated Heart Failure. *Molecular and Cellular Biology*. 2003;23(10):3593-3606. doi:10.1128/MCB.23.10.3593-3606.2003
- 62. Antos CL, McKinsey TA, Dreitz M, et al. Dose-dependent Blockade to Cardiomyocyte Hypertrophy by Histone Deacetylase Inhibitors. *Journal of Biological Chemistry*. 2003;278(31):28930-28937. doi:10.1074/jbc.M303113200
- 63. Kook H, Lepore JJ, Gitler AD, et al. Cardiac hypertrophy and histone deacetylase—dependent transcriptional repression mediated by the atypical homeodomain protein Hop. *J Clin Invest*. 2003;112(6):863-871. doi:10.1172/JCI19137
- 64. McKinsey TA, Olson EN. Cardiac histone acetylation therapeutic opportunities abound. *Trends in Genetics*. 2004;20(4):206-213. doi:10.1016/j.tig.2004.02.002
- 65. Schreiber SL, Bernstein BE. Signaling network model of chromatin. *Cell*. 2002;111(6):771-778. doi:10.1016/s0092-8674(02)01196-0
- 66. Cochran AG, Conery AR, Sims RJ. Bromodomains: a new target class for drug development. *Nat Rev Drug Discov*. 2019;18(8):609-628. doi:10.1038/s41573-019-0030-7
- 67. Shi J, Vakoc CR. The mechanisms behind the therapeutic activity of BET bromodomain inhibition. *Mol Cell*. 2014;54(5):728-736. doi:10.1016/j.molcel.2014.05.016
- 68. Dhalluin C, Carlson JE, Zeng L, He C, Aggarwal AK, Zhou MM. Structure and ligand of a histone acetyltransferase bromodomain. *Nature*. 1999;399(6735):491-496. doi:10.1038/20974
- 69. Belkina AC, Denis GV. BET domain co-regulators in obesity, inflammation and cancer. *Nat Rev Cancer*. 2012;12(7):465-477. doi:10.1038/nrc3256
- 70. Fujisawa T, Filippakopoulos P. Functions of bromodomain-containing proteins and their roles in homeostasis and cancer. *Nat Rev Mol Cell Biol*. 2017;18(4):246-262. doi:10.1038/nrm.2016.143
- 71. Vollmuth F, Blankenfeldt W, Geyer M. Structures of the Dual Bromodomains of the P-TEFb-activating Protein Brd4 at Atomic Resolution \*. *Journal of Biological Chemistry*. 2009;284(52):36547-36556. doi:10.1074/jbc.M109.033712
- 72. Jang MK, Mochizuki K, Zhou M, Jeong HS, Brady JN, Ozato K. The bromodomain protein Brd4 is a positive regulatory component of P-TEFb and stimulates RNA polymerase II-dependent transcription. *Mol Cell*. 2005;19(4):523-534. doi:10.1016/j.molcel.2005.06.027
- 73. Yang Z, He N, Zhou Q. Brd4 Recruits P-TEFb to Chromosomes at Late Mitosis To Promote G1 Gene Expression and Cell Cycle Progression. *Mol Cell Biol*. 2008;28(3):967-976. doi:10.1128/MCB.01020-07

- 74. Zhou Q, Li T, Price DH. RNA polymerase II elongation control. *Annu Rev Biochem*. 2012;81:119-143. doi:10.1146/annurev-biochem-052610-095910
- 75. Bisgrove DA, Mahmoudi T, Henklein P, Verdin E. Conserved P-TEFb-interacting domain of BRD4 inhibits HIV transcription. *Proc Natl Acad Sci U S A*. 2007;104(34):13690-13695. doi:10.1073/pnas.0705053104
- 76. Schröder S, Cho S, Zeng L, et al. Two-pronged Binding with Bromodomain-containing Protein 4 Liberates Positive Transcription Elongation Factor b from Inactive Ribonucleoprotein Complexes. *Journal of Biological Chemistry*. 2012;287(2):1090-1099. doi:10.1074/jbc.M111.282855
- 77. Jang MK, Mochizuki K, Zhou M, Jeong HS, Brady JN, Ozato K. The Bromodomain Protein Brd4 Is a Positive Regulatory Component of P-TEFb and Stimulates RNA Polymerase II-Dependent Transcription. *Molecular Cell*. 2005;19(4):523-534. doi:10.1016/j.molcel.2005.06.027
- 78. Jiang YW, Veschambre P, Erdjument-Bromage H, et al. Mammalian mediator of transcriptional regulation and its possible role as an end-point of signal transduction pathways. *Proceedings of the National Academy of Sciences*. 1998;95(15):8538-8543. doi:10.1073/pnas.95.15.8538
- 79. C Quaresma AJ, Bugai A, Barboric M. Cracking the control of RNA polymerase II elongation by 7SK snRNP and P-TEFb. *Nucleic Acids Res.* 2016;44(16):7527-7539. doi:10.1093/nar/gkw585
- 80. Lin C, Garrett AS, De Kumar B, et al. Dynamic transcriptional events in embryonic stem cells mediated by the super elongation complex (SEC). *Genes Dev.* 2011;25(14):1486-1498. doi:10.1101/gad.2059211
- 81. Lin C, Smith ER, Takahashi H, et al. AFF4, a component of the ELL/P-TEFb elongation complex and a shared subunit of MLL chimeras, can link transcription elongation to leukemia. *Mol Cell*. 2010;37(3):429-437. doi:10.1016/j.molcel.2010.01.026
- 82. Altendorfer E, Mochalova Y, Mayer A. BRD4: a general regulator of transcription elongation. *Transcription*. 2022;13(1-3):70-81. doi:10.1080/21541264.2022.2108302
- 83. Gupta VK, Sigrist SJ. Sperm(idine) answers the next generation. *Cell Cycle*. 2013;12(4):542-542. doi:10.4161/cc.23676
- 84. Hajmirza A, Emadali A, Gauthier A, Casasnovas O, Gressin R, Callanan MB. BET Family Protein BRD4: An Emerging Actor in NFκB Signaling in Inflammation and Cancer. *Biomedicines*. 2018;6(1):16. doi:10.3390/biomedicines6010016
- 85. Huang B, Yang XD, Zhou MM, Ozato K, Chen LF. Brd4 Coactivates Transcriptional Activation of NF-κB via Specific Binding to Acetylated RelA. *Molecular and Cellular Biology*. 2009;29(5):1375. doi:10.1128/MCB.01365-08

- 86. Stratton MS, Bagchi RA, Felisbino MB, et al. Dynamic Chromatin Targeting of BRD4 Stimulates Cardiac Fibroblast Activation. *Circ Res.* 2019;125(7):662-677. doi:10.1161/CIRCRESAHA.119.315125
- 87. Fang M, Luo J, Zhu X, Wu Y, Li X. BRD4 Silencing Protects Angiotensin II-Induced Cardiac Hypertrophy by Inhibiting TLR4/NF-κB and Activating Nrf2-HO-1 Pathways. Ali Sheikh MS, ed. *Cardiology Research and Practice*. 2022;2022:1-11. doi:10.1155/2022/8372707
- 88. Liu W, Ma Q, Wong K, et al. Brd4 and JMJD6-associated anti-pause enhancers in regulation of transcriptional pause release. *Cell*. 2013;155(7):1581-1595. doi:10.1016/j.cell.2013.10.056
- 89. Rahman S, Sowa ME, Ottinger M, et al. The Brd4 extraterminal domain confers transcription activation independent of pTEFb by recruiting multiple proteins, including NSD3. *Mol Cell Biol*. 2011;31(13):2641-2652. doi:10.1128/MCB.01341-10
- 90. Wu SY, Lee AY, Lai HT, Zhang H, Chiang CM. Phospho switch triggers Brd4 chromatin binding and activator recruitment for gene-specific targeting. *Mol Cell*. 2013;49(5):843-857. doi:10.1016/j.molcel.2012.12.006
- 91. BRD4 and Cancer: going beyond transcriptional regulation | Molecular Cancer | Full Text. Accessed September 13, 2024. https://molecular-cancer.biomedcentral.com/articles/10.1186/s12943-018-0915-9
- 92. Donner AJ, Ebmeier CC, Taatjes DJ, Espinosa JM. CDK8 is a positive regulator of transcriptional elongation within the serum response network. *Nature Structural & Molecular Biology*. 2010;17(2):194-201. doi:10.1038/nsmb.1752
- 93. Mammalian mediator of transcriptional regulation and its possible role as an end-point of signal transduction pathways | PNAS. Accessed September 12, 2024. https://www.pnas.org/doi/abs/10.1073/pnas.95.15.8538
- 94. Wu SY, Chiang CM. The Double Bromodomain-containing Chromatin Adaptor Brd4 and Transcriptional Regulation\*. *Journal of Biological Chemistry*. 2007;282(18):13141-13145. doi:10.1074/jbc.R700001200
- 95. Bhagwat AS, Roe JS, Mok BYL, Hohmann AF, Shi J, Vakoc CR. BET Bromodomain Inhibition Releases the Mediator Complex from Select *cis*-Regulatory Elements. *Cell Reports*. 2016;15(3):519-530. doi:10.1016/j.celrep.2016.03.054
- 96. Allen BL, Taatjes DJ. The Mediator complex: a central integrator of transcription. *Nat Rev Mol Cell Biol*. 2015;16(3):155-166. doi:10.1038/nrm3951
- 97. Yang CY, Qin C, Bai L, Wang S. Small-molecule PROTAC degraders of the Bromodomain and Extra Terminal (BET) proteins A review. *Drug Discovery Today: Technologies*. 2019;31:43-51. doi:10.1016/j.ddtec.2019.04.001

- 98. Lovén J, Hoke HA, Lin CY, et al. Selective Inhibition of Tumor Oncogenes by Disruption of Super-Enhancers. *Cell.* 2013;153(2):320-334. doi:10.1016/j.cell.2013.03.036
- 99. Chiang CM. Brd4 engagement from chromatin targeting to transcriptional regulation: selective contact with acetylated histone H3 and H4. *F1000 Biol Rep.* 2009;1:98. doi:10.3410/B1-98
- 100. Alqahtani A, Choucair K, Ashraf M, et al. Bromodomain and extra-terminal motif inhibitors: a review of preclinical and clinical advances in cancer therapy. *Future Sci OA*. 2019;5(3):FSO372. doi:10.4155/fsoa-2018-0115
- 101. Hewings DS, Rooney TPC, Jennings LE, et al. Progress in the Development and Application of Small Molecule Inhibitors of Bromodomain–Acetyl-lysine Interactions. *J Med Chem.* 2012;55(22):9393-9413. doi:10.1021/jm300915b
- 102. Filippakopoulos P, Qi J, Picaud S, et al. Selective inhibition of BET bromodomains. *Nature*. 2010;468(7327):1067-1073. doi:10.1038/nature09504
- 103. Nicodeme E, Jeffrey KL, Schaefer U, et al. Suppression of inflammation by a synthetic histone mimic. *Nature*. 2010;468(7327):1119-1123. doi:10.1038/nature09589
- 104. Duan Q, McMahon S, Anand P, et al. BET bromodomain inhibition suppresses innate inflammatory and profibrotic transcriptional networks in heart failure. *Sci Transl Med*. 2017;9(390):eaah5084. doi:10.1126/scitranslmed.aah5084
- 105. Delmore J, Issa GC, Issa GC, et al. BET Bromodomain Inhibition as a Therapeutic Strategy to Target c-Myc. *Cell*. 2011;146(6):904-917. doi:10.1016/j.cell.2011.08.017
- 106. Puissant A, Frumm SM, Alexe G, et al. Targeting MYCN in neuroblastoma by BET bromodomain inhibition. *Cancer Discov.* 2013;3(3):308-323. doi:10.1158/2159-8290.CD-12-0418
- 107. Klein K, Kabala PA, Grabiec AM, et al. The bromodomain protein inhibitor I-BET151 suppresses expression of inflammatory genes and matrix degrading enzymes in rheumatoid arthritis synovial fibroblasts. *Ann Rheum Dis.* 2016;75(2):422-429. doi:10.1136/annrheumdis-2014-205809
- 108. Anand P, Brown JD, Lin CY, et al. BET bromodomains mediate transcriptional pause release in heart failure. *Cell.* 2013;154(3):569-582. doi:10.1016/j.cell.2013.07.013
- 109. Spiltoir JI, Stratton MS, Cavasin MA, et al. BET acetyl-lysine binding proteins control pathological cardiac hypertrophy. *J Mol Cell Cardiol*. 2013;63:175-179. doi:10.1016/j.yjmcc.2013.07.017
- 110. Devaiah BN, Lewis BA, Cherman N, et al. BRD4 is an atypical kinase that phosphorylates serine2 of the RNA polymerase II carboxy-terminal domain. *Proc Natl Acad Sci U S A*. 2012;109(18):6927-6932. doi:10.1073/pnas.1120422109

- 111. Lovén J, Hoke HA, Lin CY, et al. Selective inhibition of tumor oncogenes by disruption of super-enhancers. *Cell.* 2013;153(2):320-334. doi:10.1016/j.cell.2013.03.036
- 112. Stratton MS, Lin CY, Anand P, et al. Signal-Dependent Recruitment of BRD4 to Cardiomyocyte Super-Enhancers Is Suppressed by a MicroRNA. *Cell Reports*. 2016;16(5):1366-1378. doi:10.1016/j.celrep.2016.06.074
- 113. Martin RD, Sun Y, Bourque K, et al. Receptor- and cellular compartment-specific activation of the cAMP/PKA pathway by α1-adrenergic and ETA endothelin receptors. *Cell Signal*. 2018;44:43-50. doi:10.1016/j.cellsig.2018.01.002
- 114. Gallego M, Setién R, Puebla L, Boyano-Adánez MDC, Arilla E, Casis O. alpha1-Adrenoceptors stimulate a Galphas protein and reduce the transient outward K+ current via a cAMP/PKA-mediated pathway in the rat heart. *Am J Physiol Cell Physiol*. 2005;288(3):C577-585. doi:10.1152/ajpcell.00124.2004
- 115. Horie K, Itoh H, Tsujimoto G. Hamster alpha 1B-adrenergic receptor directly activates Gs in the transfected Chinese hamster ovary cells. *Mol Pharmacol*. 1995;48(3):392-400.
- 116. Ruan Y, Kan H, Parmentier JH, Fatima S, Allen LF, Malik KU. Alpha-1A adrenergic receptor stimulation with phenylephrine promotes arachidonic acid release by activation of phospholipase D in rat-1 fibroblasts: inhibition by protein kinase A. *J Pharmacol Exp Ther*. 1998;284(2):576-585.
- 117. Shibata K, Katsuma S, Koshimizu T, et al. alpha 1-Adrenergic receptor subtypes differentially control the cell cycle of transfected CHO cells through a cAMP-dependent mechanism involving p27Kip1. *J Biol Chem.* 2003;278(1):672-678. doi:10.1074/jbc.M201375200
- 118. Sano M, Abdellatif M, Oh H, et al. Activation and function of cyclin T-Cdk9 (positive transcription elongation factor-b) in cardiac muscle-cell hypertrophy. *Nat Med*. 2002;8(11):1310-1317. doi:10.1038/nm778
- 119. Martin RD, Sun Y, MacKinnon S, et al. Differential Activation of P-TEFb Complexes in the Development of Cardiomyocyte Hypertrophy following Activation of Distinct G Protein-Coupled Receptors. *Mol Cell Biol*. 2020;40(14):e00048-20. doi:10.1128/MCB.00048-20
- 120. Armbruster BN, Li X, Pausch MH, Herlitze S, Roth BL. Evolving the lock to fit the key to create a family of G protein-coupled receptors potently activated by an inert ligand. *Proc Natl Acad Sci USA*. 2007;104(12):5163-5168. doi:10.1073/pnas.0700293104
- 121. Zhu H, Roth BL. DREADD: A Chemogenetic GPCR Signaling Platform. *International Journal of Neuropsychopharmacology*. 2015;18(1):pyu007-pyu007. doi:10.1093/ijnp/pyu007

- 122. Thompson KJ, Khajehali E, Bradley SJ, et al. DREADD Agonist 21 Is an Effective Agonist for Muscarinic-Based DREADDs *in Vitro* and *in Vivo*. *ACS Pharmacol Transl Sci*. 2018;1(1):61-72. doi:10.1021/acsptsci.8b00012
- 123. Wess J, Nakajima K, Jain S. Novel designer receptors to probe GPCR signaling and physiology. *Trends Pharmacol Sci.* 2013;34(7):385-392. doi:10.1016/j.tips.2013.04.006
- 124. Zhang S, Gumpper RH, Huang XP, et al. Molecular basis for selective activation of DREADD-based chemogenetics. *Nature*. 2022;612(7939):354-362. doi:10.1038/s41586-022-05489-0
- 125. Wess J. Designer GPCRs as Novel Tools to Identify Metabolically Important Signaling Pathways. *Front Endocrinol*. 2021;12:706957. doi:10.3389/fendo.2021.706957
- 126. Roth BL. DREADDs for Neuroscientists. *Neuron*. 2016;89(4):683-694. doi:10.1016/j.neuron.2016.01.040
- 127. The DREADD agonist clozapine N-oxide (CNO) is reverse-metabolized to clozapine and produces clozapine-like interoceptive stimulus effects in rats and mice PMC. Accessed August 24, 2024. https://www.ncbi.nlm.nih.gov/pmc/articles/PMC5832819/
- 128. Gomez JL, Bonaventura J, Lesniak W, et al. Chemogenetics revealed: DREADD occupancy and activation via converted clozapine. *Science*. 2017;357(6350):503-507. doi:10.1126/science.aan2475
- 129. Nagai Y, Miyakawa N, Takuwa H, et al. Deschloroclozapine, a potent and selective chemogenetic actuator enables rapid neuronal and behavioral modulations in mice and monkeys. *Nat Neurosci*. 2020;23(9):1157-1167. doi:10.1038/s41593-020-0661-3
- 130. Phillips ST, de Paulis T, Baron BM, et al. Binding of 5H-Dibenzo[b,e][1,4]diazepine and Chiral 5H-Dibenzo[a,d]cycloheptene Analogs of Clozapine to Dopamine and Serotonin Receptors. *J Med Chem.* 1994;37(17):2686-2696. doi:10.1021/jm00043a008
- 131. Effect of chemogenetic actuator drugs on prefrontal cortex-dependent working memory in nonhuman primates | Neuropsychopharmacology. Accessed August 24, 2024. https://www.nature.com/articles/s41386-020-0660-9
- 132. Armbruster BN, Li X, Pausch MH, Herlitze S, Roth BL. Evolving the lock to fit the key to create a family of G protein-coupled receptors potently activated by an inert ligand. *Proc Natl Acad Sci USA*. 2007;104(12):5163-5168. doi:10.1073/pnas.0700293104
- 133. Lukasheva V, Devost D, Le Gouill C, et al. Signal profiling of the β1AR reveals coupling to novel signalling pathways and distinct phenotypic responses mediated by β1AR and β2AR. *Sci Rep.* 2020;10(1):8779. doi:10.1038/s41598-020-65636-3
- 134. Namkung Y, LeGouill C, Kumar S, et al. Functional selectivity profiling of the angiotensin II type 1 receptor using pathway-wide BRET signaling sensors. *Sci Signal*. 2018;11(559):eaat1631. doi:10.1126/scisignal.aat1631

- 135. Chen S. Ultrafast one-pass FASTQ data preprocessing, quality control, and deduplication using fastp. *iMeta*. 2023;2(2):e107. doi:10.1002/imt2.107
- 136. Piper MM Bob Freeman, Mary. Alignment with STAR. Introduction to RNA-Seq using high-performance computing ARCHIVED. June 7, 2017. Accessed December 7, 2024. https://hbctraining.github.io/Intro-to-rnaseq-hpc-O2/lessons/03\_alignment.html
- 137. Intro-to-rnaseq-hpc-salmon-flipped/lessons/QC\_STAR\_and\_Qualimap\_run.md at main hbctraining/Intro-to-rnaseq-hpc-salmon-flipped. GitHub. Accessed December 7, 2024. https://github.com/hbctraining/Intro-to-rnaseq-hpc-salmon-flipped/blob/main/lessons/QC\_STAR\_and\_Qualimap\_run.md
- 138. Accessed December 7, 2024. https://subread.sourceforge.net/featureCounts.html
- 139. Love MI, Huber W, Anders S. Moderated estimation of fold change and dispersion for RNA-seq data with DESeq2. *Genome Biol.* 2014;15(12):550. doi:10.1186/s13059-014-0550-8
- 140. clusterProfiler/R/enrichGO.R at devel · YuLab-SMU/clusterProfiler. GitHub. Accessed December 7, 2024. https://github.com/YuLab-SMU/clusterProfiler/blob/devel/R/enrichGO.R
- 141. KEGG PATHWAY Database. Accessed December 7, 2024. https://www.genome.jp/kegg/pathway.html
- 142. Zhang JD, Wiemann S. KEGGgraph: a graph approach to KEGG PATHWAY in R and bioconductor. *Bioinformatics*. 2009;25(11):1470-1471. doi:10.1093/bioinformatics/btp167
- 143. Transcription factor activity inference in bulk RNA-seq. Accessed October 10, 2024. https://www.bioconductor.org/packages/release/bioc/vignettes/decoupleR/inst/doc/tf\_bk.ht ml#5 Visualization
- 144. Winter GE, Mayer A, Buckley DL, et al. BET Bromodomain Proteins Function as Master Transcription Elongation Factors Independent of CDK9 Recruitment. *Mol Cell*. 2017;67(1):5-18.e19. doi:10.1016/j.molcel.2017.06.004
- 145. Mertz JA, Conery AR, Bryant BM, et al. Targeting MYC dependence in cancer by inhibiting BET bromodomains. *Proc Natl Acad Sci USA*. 2011;108(40):16669-16674. doi:10.1073/pnas.1108190108
- 146. Ai N, Hu X, Ding F, et al. Signal-induced Brd4 release from chromatin is essential for its role transition from chromatin targeting to transcriptional regulation. *Nucleic Acids Research*. 2011;39(22):9592-9604. doi:10.1093/nar/gkr698
- 147. Bartholomeeusen K, Xiang Y, Fujinaga K, Peterlin BM. Bromodomain and Extra-terminal (BET) Bromodomain Inhibition Activate Transcription via Transient Release of Positive Transcription Elongation Factor b (P-TEFb) from 7SK Small Nuclear Ribonucleoprotein \*.

- *Journal of Biological Chemistry*. 2012;287(43):36609-36616. doi:10.1074/jbc.M112.410746
- 148. Francisco JC, Dai Q, Luo Z, et al. Transcriptional Elongation Control of Hepatitis B Virus Covalently Closed Circular DNA Transcription by Super Elongation Complex and BRD4. *Molecular and Cellular Biology*. 2017;37(19):e00040-17. doi:10.1128/MCB.00040-17
- 149. Li Z, Guo J, Wu Y, Zhou Q. The BET bromodomain inhibitor JQ1 activates HIV latency through antagonizing Brd4 inhibition of Tat-transactivation. *Nucleic Acids Research*. 2013;41(1):277-287. doi:10.1093/nar/gks976
- 150. Lukasheva V, Devost D, Le Gouill C, et al. Signal profiling of the β1AR reveals coupling to novel signalling pathways and distinct phenotypic responses mediated by β1AR and β2AR. *Sci Rep.* 2020;10(1):8779. doi:10.1038/s41598-020-65636-3
- 151. Wu SY, Lee AY, Hou SY, et al. Brd4 links chromatin targeting to HPV transcriptional silencing. *Genes Dev.* 2006;20(17):2383-2396. doi:10.1101/gad.1448206
- 152. Guettier JM, Gautam D, Scarselli M, et al. A chemical-genetic approach to study G protein regulation of β cell function in vivo. *Proc Natl Acad Sci USA*. 2009;106(45):19197-19202. doi:10.1073/pnas.0906593106
- 153. Black JB, Premont RT, Daaka Y. Feedback regulation of G protein-coupled receptor signaling by GRKs and arrestins. *Seminars in Cell & Developmental Biology*. 2016;50:95-104. doi:10.1016/j.semcdb.2015.12.015
- 154. Gainetdinov RR, Premont RT, Bohn LM, Lefkowitz RJ, Caron MG. DESENSITIZATION OF G PROTEIN–COUPLED RECEPTORS AND NEURONAL FUNCTIONS. *Annu Rev Neurosci*. 2004;27(1):107-144. doi:10.1146/annurev.neuro.27.070203.144206
- 155. Scarselli M, Donaldson JG. Constitutive Internalization of G Protein-coupled Receptors and G Proteins via Clathrin-independent Endocytosis. *Journal of Biological Chemistry*. 2009;284(6):3577-3585. doi:10.1074/jbc.M806819200
- 156. Liu L, Yang C, Candelario-Jalil E. Role of BET Proteins in Inflammation and CNS Diseases. *Front Mol Biosci.* 2021;8:748449. doi:10.3389/fmolb.2021.748449
- 157. Filippakopoulos P, Qi J, Picaud S, et al. Selective inhibition of BET bromodomains. *Nature*. 2010;468(7327):1067-1073. doi:10.1038/nature09504
- 158. Baud MGJ, Lin-Shiao E, Cardote T, et al. A bump-and-hole approach to engineer controlled selectivity of BET bromodomain chemical probes. *Science*. 2014;346(6209):638-641. doi:10.1126/science.1249830
- 159. Zhang H, Dhalla NS. The Role of Pro-Inflammatory Cytokines in the Pathogenesis of Cardiovascular Disease. *IJMS*. 2024;25(2):1082. doi:10.3390/ijms25021082